Sequence Programmable Peptoid Polymers for Diverse Materials Applications

*Abigail S. Knight, Effie Y. Zhou, Matthew B. Francis, and Ronald N. Zuckermann**

Polymer sequence programmability is required for the diverse structures and complex properties that are achieved by native biological polymers, but efforts towards controlling the sequence of synthetic polymers are, by comparison, still in their infancy. Traditional polymers provide robust and chemically diverse materials, but synthetic control over their monomer sequences is limited. The modular and step-wise synthesis of peptoid polymers, on the other hand, allows for precise control over the monomer sequences, affording opportunities for these chains to fold into well-defined nanostructures. Hundreds of different side chains have been incorporated into peptoid polymers using efficient reaction chemistry, allowing for a seemingly infinite variety of possible synthetically accessible polymer sequences. Combinatorial discovery techniques have allowed the identification of functional polymers within large libraries of peptoids, and newly developed theoretical modeling tools specifically adapted for peptoids enable the future design of polymers with desired functions. Work towards controlling the three-dimensional structure of peptoids, from the conformation of the amide bond to the formation of protein-like tertiary structure, has and will continue to enable the construction of tunable and innovative nanomaterials that bridge the gap between natural and synthetic polymers.

1. Introduction

The challenge of creating synthetic materials with the structural sophistication and complex function found in biology has been a long-term goal in materials science (**Figure 1**). Research from both the biological and chemical communities has been converging to fill the large gap between synthetic homopolymers and native biological materials. Nature has evolved a variety of sequence programmable polymers that have functions ranging from carrying the genetic code to catalyzing chemical reactions. Natural biopolymers represent the pinnacle of sequence control, and this has allowed for the evolution of a plethora of sophisticated functions. These functions are enabled by the precision control of molecular interactions on the ångström scale – the length scale of individual bonds. Proteins have complex networks of noncovalent interactions that are necessary for specific molecular recognition (e.g. binding to specific DNA sequences), as well as precisely placed functional groups that are required for catalysis. These exquisite nanoscale architectures are typically folded from absolutely monodisperse linear polymer chains of a precisely defined monomer sequence. Biological research has been moving towards the production of novel materials using the natural biosynthetic machinery; recent work in directed protein evolution[1] and the incorporation of unnatural amino acids[2–4] has made it possible to evolve proteins for non-native functions. However, biopolymers and materials based on proteins or DNA suffer from inherent limitations, including the necessity of water as their solvent, susceptibility to enzymatic degradation, and poor environmental stability to variation in temperature, pH, and ionic strength.

The study of synthetic polymeric materials began with homopolymers and copolymers, and has expanded into functional heteropolymers. While polymeric materials tend to be significantly more robust than protein-based materials, they lack the structural sophistication achieved by proteins. In recent years, polymer chemists have sought to improve synthesis methods to emulate biology's degree of sequence control, and the gap between synthetic polymers and native biological materials is beginning to close.[5–7] Many synthetic strategies for polymer sequence control have recently been developed, including templating, kinetic control, orthogonal reactivities, and the linking of structures after polymerization.[5] These techniques have allowed for significant advances in synthetic polymer materials, especially in the development of novel photonics and dynamic materials.[7–9] The demonstrated utility of partial sequence control illuminates the abundance of opportunities available as the synthetic tools for precise monomer control continue to improve.

Step-wise synthesis provides the opportunity to generate polymers with complete sequence control. This strategy was pioneered using solid supports by Merrifield for peptide synthesis,[10] but has also been developed for the synthesis of DNA, RNA and a variety of resin-bound organic structures.[11]

A. S. Knight, E. Y. Zhou, Prof. M. B. Francis
UC Berkeley Chemistry Department
Latimer Hall, Berkeley, CA 94720, USA
Dr. R. N. Zuckermann, Prof. M. B. Francis
The Molecular Foundry
Lawrence Berkeley National Lab
1 Cyclotron Road, Berkeley, CA 94720, USA
E-mail: rnzuckermann@lbl.gov

DOI: 10.1002/adma.201500275

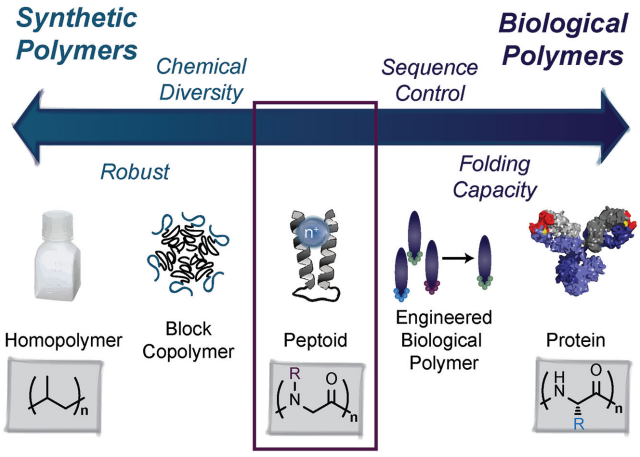

Figure 1. The range of characteristics for synthetic and biological polymers reveals a gap that is strategically filled by peptoid-based materials.

However, the extension of these techniques to create sequence-defined non-natural polymers of significant main chain lengths has been a longstanding challenge. The monomer coupling reactions used to make such polymers need to have nearly quantitative yields in order to synthesize large, well-defined polymer chains. Peptidomimetic *N*-substituted glycine polymers, or peptoids, break this yield barrier and have thus opened up a new class of sequence-defined polymers (**Figure 2**).[12] Peptoid polymers thus straddle the boundary between biological materials and synthetic polymers: their biomimetic structure and precision sequence control provides a breadth of opportunities to produce sequence programmable, folded polymers with the robustness typical of synthetic materials.

The step-wise solid-phase synthesis of peptoids was developed in 1992,[13] and since then their application to various fields has grown exponentially. This synthesis strategy provides access to an almost infinite diversity of polymer sequences, since each monomer is individually tunable. The large population of potential polymers opens the opportunity to screen for particular sequences with new functionalities using combinatorial chemistry.[14] Moreover, the ability to identify functional structures from such libraries accelerates the discovery of materials with advanced properties. Although this capability exists with genetically-specified biological polymers (e.g., polypeptides and polynucleotides), peptoids are a more versatile option due to their increased chemical diversity, increased stability to degradative enzymes and environmental variables, and

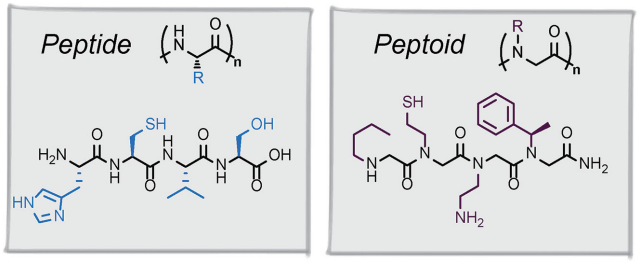

Figure 2. Peptide versus peptoid structure. Example tetramers are shown of each.

Abigail Knight received her B.S. in chemistry from the University of North Carolina, Chapel Hill in 2010 and is currently finishing her Ph.D at the University of California, Berkeley under the guidance of Professor Matthew Francis. After the completion of her Ph.D. she will begin a postdoctoral position at the University of California, Santa Barbara with Professor Craig Hawker. Her research interests include bioinspired materials and selective metal coordination.

Effie Zhou recently completed her B.S. in chemistry at the University of California at Berkeley working in the laboratory of Matthew Francis. She is interested in working at the interface of chemistry and biology in her future research career.

Matthew Francis received his B.S. in Chemistry from Miami University, and he received his Ph.D. from Harvard University working with Prof. Eric Jacobsen. He was a Postdoctoral Fellow with Prof. Jean Fréchet through the Miller Institute for Basic Research in Science at UC Berkeley, and he started his independent career in the UC Berkeley Chemistry Department in 2001. He has built a research program involving the development of new reactions for protein modification. These new chemical tools have then been used to generate complex biomolecular assemblies for use in in vivo delivery, light harvesting, and water treatment applications.

Ronald Zuckermann is a Sr. Scientist and Facility Director of the Biological Nanostructures Facility at the Molecular Foundry at the Lawrence Berkeley National Laboratory. He obtained a Ph.D. in Chemistry from UC Berkeley in 1989, and worked as a research scientist in the biotechnology industry for 16 years developing combinatorial drug discovery technologies. He was named a Chiron Research Fellow in 2003, and an LBNL Sr. Scientist in 2011. He invented sequence-defined peptoid polymers, and works on folding them into precise nanoscale architectures. He adapts structural design rules from biology and applies them to the world of materials science.
From left to right: R.Z., M.F., A.K., and E.Z.

Adv. Mater. **2015**,
DOI: 10.1002/adma.201500275

a decreased synthetic cost. The step-wise synthesis of peptoid polymers makes the nearly absolute monodispersity encountered with biological polymers accessible, allowing for unique structural control in a synthetic polymer. Recent reviews have described applications of peptoids as small molecules[15–17] and polymers,[18–22] and in the field of biomaterials.[12,23] This review aims to highlight the unique applications of peptoids as modular and tunable structures with the potential to bridge the gap between synthetic and biological polymers in the future of bioinspired materials research.

2. Synthesis and Structural Control of Peptoids

2.1. Synthesis

Peptoid polymers have been synthesized using two strategies: an iterative step-wise technique, typically performed on a solid support, that allows precise control of sequence definition, and a polymerization approach, typically completed in solution, that allows access to higher molecular weight polymers. The step-wise submonomer synthesis uses a two-step monomer addition cycle, similar to solid-phase peptide synthesis (**Figure 3**a).[24] Both reactions used in the submomoner synthesis strategy can achieve near quantitative yields, allowing the efficient synthesis of virtually monodisperse sequence-defined polymers. This synthesis, which can be performed manually or by an automated synthesizer, can yield polymers of up to fifty monomer units in length. For larger polymers, the ring-opening polymerization (ROP) of *N*-substituted α-amino acid-*N*-carboxyanhydrides (*N*-substituted NCAs) has been applied to create peptoid homopolymers and copolymers (Figure 3b). [22] Less sequence control is available with the polymerization approach, but a large number of different side chains have been incorporated, providing access to a wide variety of polymer structures within the same backbone.

To access sequence-defined peptoid polymers, a step-wise modular synthesis is required. Although the iterative synthesis appears tedious and time consuming in comparison, both synthesis on a solid-support and the automation of the coupling reactions enables rapid and facile synthesis of these polymers. The nearly quantitative yields of the two-step synthesis lead to high yields of very pure polymer material. The modular synthesis begins with the acylation of a resin-bound amine with a haloacetic acid, followed by displacement of the halogen with a primary amine (Figure 3a). The nature of this synthesis allows for the use of diverse functional groups as side chains, since nearly any primary amine can be incorporated as a submonomer. Unlike the synthetic strategies used for the synthesis of biological polymers, this synthetic scheme does not require the synthesis of special building blocks. Correspondingly, hundreds of side chains can be easily incorporated at each position directly from commercially available materials. Side chains with reactive functional groups necessitate protection, but many heterocycles can be used directly with no protection.[25]

Since the first demonstration of the submonomer synthesis technique,[24] hundreds of monomers including ionic, aromatic, heterocyclic, and aliphatic moieties have been incorporated.[26] Almost any primary amine can perform the halogen

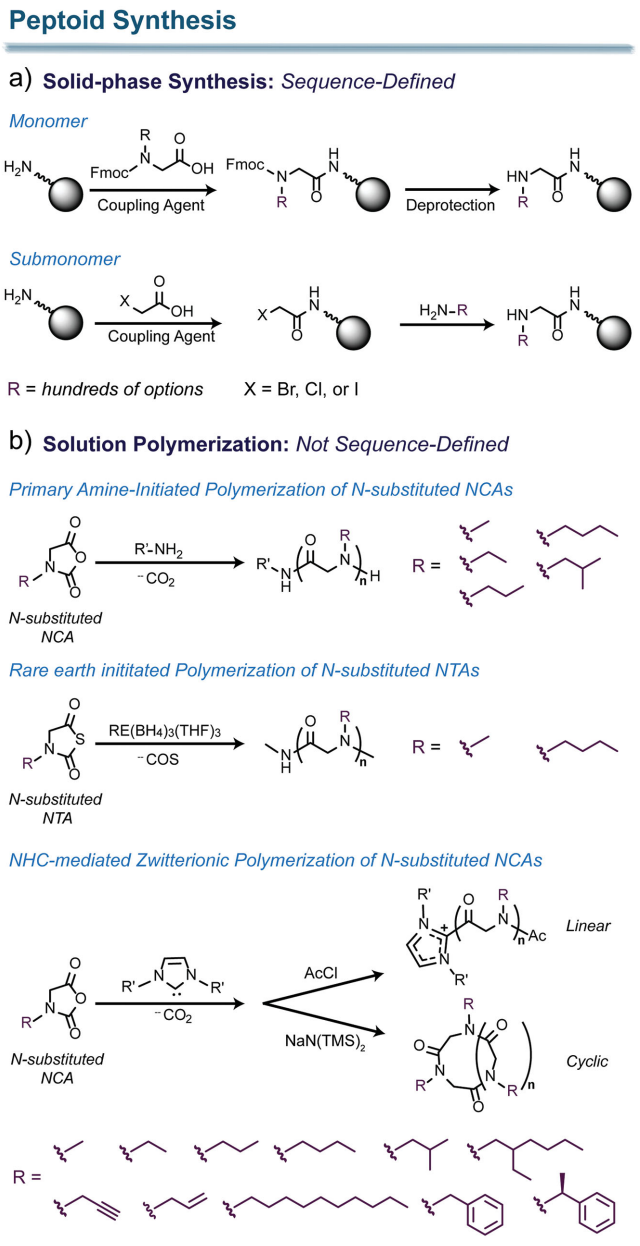

Figure 3. An outline of the most common techniques used for the synthesis of α-peptoids. a) Peptoid synthesis techniques used with solid-phase polystyrene resins. Carbodiimides are most commonly used as the coupling agent and piperidine is commonly used for the deprotection step. b) Solution polymerization using *N*-substituted NCAs and NTAs for peptoid polymer synthesis. For $RE(BH_4)_3(THF)_3$, the rare earth (RE) can be Sc, Y, La, Nd, Dy, or Lu.

displacement, providing an unlimited library of functional groups. Functional groups that have been incorporated on the side chains range from small aliphatic groups, to amino acid-like side chains, to larger moieties (e.g., carbohydrates, dyes, and cofactors) and individual side chains have been demonstrated to contribute significantly to polymer properties and function. A few examples include azobenzene side chains that lead to photoresponsive polymers[27] and chiral monomers that introduce entropic constraints and promote the formation of

secondary structures.[28] The submonomer synthesis method has also been expanded to include chemoselective coupling partners, such as ketones, aldehydes, and thiols, for conjugation of peptoid polymers to other molecules or to substrates.[29] Additionally, Kirshenbaum et al. demonstrated the incorporation of larger moieties, including hormones and metal complexes, which were added to a fully elongated peptoid using click chemistry.[30] Their work compared the electrochemical properties of ferrocene-peptoid conjugates to the properties of free ferrocene, noting a minimal attenuation of electrochemical properties.

While traditional synthetic techniques allow for rapid and facile synthesis of peptoid polymers, methods relying on biosynthetic pathways could increase the ease of synthesis and enable larger sequence-defined peptoid polymers to be formed. The current techniques only produce small oligomers, but these strategies have huge potential. A ribosomal synthesis has been described for the synthesis of peptoids and peptide-peptoid hybrids by the Suga group.[31] A cell-free translation system was used[32] in addition to flexizymes – artificial aminoacyl-tRNA ribozymes[33] – allowing for the incorporation of *N*-substituted glycines. A variety of functional groups were evaluated, including branched and unbranched alkyl chains and functional chains such as esters, azides, alkenes, and alkynes. Although the yields were low, linear peptoids of up to six monomers were synthesized in addition to cyclic peptide-peptoid hybrids linked with a thioether. Biological machinery has also been applied to the synthesis β-peptoid homopolymers; a lipase was employed to catalyze the synthesis of poly(*N*-(2-hydroxyethyl)-β-propylamide.[34] The synthesis of hexamers was characterized by MALDI-TOF MS, and the structure was further derivatized to form a brush with polycaprolactone. The copolymer was cast to form films of microstructures characterized by SEM. Although all of the peptoids that have been synthesized with biological machinery are limited in length, these groups have opened up the avenue for enzyme-based synthesis of peptoid-polymers.

A variety of combinatorial platforms using the submonomer synthesis have been developed and employed for identifying functional peptoid sequences. Libraries were initially developed for drug discovery applications such as finding low molecular weight structures that bind specifically to a protein.[35] They have since been used for additional applications including identifying antimicrobial[36] and antifouling[37] molecules and ligands for selective metal coordination.[38] The strength of the combinatorial approach is the ability to screen thousands of molecules for a particular functionality, but once the active compound is identified the structure must be removed from the resin to identify the sequence. Therefore, a cleavable linker such as a methionine (cleavable with CNBr) or a photocleavable linker must be incorporated. Once the peptoid is cleaved, the structure is typically identified using tandem mass spectrometry (MS-MS). In particular, the Kodadek group has contributed to the body of methods for synthesis and screening of combinatorial peptoid libraries. Techniques that could be applied to materials applications include the design of dimeric[39] and cyclic[40] peptoid libraries that can be sequenced with MS-MS and the development of a two-color quantum dot-based screen.[39] Their work has additionally highlighted the utility of redundant combinatorial libraries to eliminate false positives before post-screening validation.[41] Combinatorial techniques have been applied not only on polystyrene-based resins, but additionally on glass slides[42] and cellulose;[43] this diversity of substrates allows for the development of novel materials such as microarrays that have been used to identify substrates for the early detection of diseases.[44]

While step-wise synthesis is required for sequence control of peptoid polymers and enables the application of combinatorial chemistry, there are still limitations in the length of the polymers that can be accessed. Techniques using traditional living polymerizations have been developed to overcome this limitation. The ring-opening polymerization of *N*-substituted NCAs to form polysarcosine was initially performed in the 1926.[45] In more recent research efforts, the Luxenhofer group has synthesized a variety of polypeptoids using the ROP of *N*-substituted NCAs (Figure 3b). They have demonstrated the reliability of living polymerization by making well controlled homopolymers and multiblock copolymers. These copolymers are not accessible via the ROP of NCAs without the *N*-substitution due to irreversible chain termination.[46] Polymerization of *N*-substituted NCAs leads to high monomer conversion and yields polymers with molecular weights of approximately 1 – 10 kg/mol[47] and low polydispersity index ($Đ_M$) values (below 1.1).[48] The polymers are flexible and have a diversity of side chains. Aliphatic side chains with one to four carbons have been evaluated; polymers with shorter side-chains were determined to be water-soluble and those with longer chains were insoluble in water. This allowed for the design of amphiphilic block copolymers. The polymers were characterized by matrix-assisted laser desorption/ionization time of flight mass spectrometry (MALDI-TOF MS), NMR, and GPC. The kinetics of the polymerization were determined to be pseudo first-order with respect to the initiator, allowing for predictable molecular weights.

A few variants of the ring-opening polymerization of *N*-substituted NCAs have also been explored. Zhang and coworkers have described the polymerization of *N*-substituted NCAs using *N*-heterocyclic carbene-mediated ROP (Figure 3b), which interestingly can yield either linear or cyclic polymers.[49] The synthesis of the cyclic polymers was determined to proceed with pseudo-first order kinetics and lead to high monomer conversions with narrow weight distributions ($Đ_M$ = 1.03 – 1.15).[50] Cyclic poly(*N*-decylglycine)s were synthesized with an impressive range of molecular weights (4.8 – 31 kg/mol). Block copolymers were synthesized with poly(*N*-methylglycine) achieving similar monomer conversion yields. These block-copolymers were demonstrated to form spherical micelles that transitioned in tubular micelles over time. Ling et al. used a *N*-substituted glycine *N*-thiocarboxyanhydrides (*N*-substituted NTA), a thio-variant of the *N*-substituted NCAs, to synthesize hydrophilic polymers with sarcosine monomers,[51] hydrophobic polymers with butyl side-chains, and block copolymers which are thermoresponsive.[52] The *N*-substituted NTAs are simpler to synthesize than the corresponding *N*-substituted NCAs and are stable for up to a year at room temperature in an inert atmosphere. Polymerizations of *N*-substituted NTAs required higher temperatures due to lower reactivity, however, the yields, molecular weights, and polydispersities of the synthesized polymers are comparable to those polymerized from *N*-substituted NCAs.

Adv. Mater. **2015**,
DOI: 10.1002/adma.201500275

Critical to the development of functional peptoid-based materials is the ability to immobilize peptoid polymers on various surfaces. There are two fundamental approaches to this: synthesizing polymers from a substrate surface, and ligating structures to a surface after synthesis. Examples of synthesizing polymers directly from a substrate include synthesis on glass surfaces[42,53] and living polymerization on a 1% crosslinked polystyrene beaded solid-support, which is commonly used for solid-phase synthesis.[47] Photolithographic synthesis has been reported using UV-irradiation to unmask a protected surface moiety, allowing spatial and density control over step-wise peptoid synthesis on a glass surface.[42] Additionally, amphiphilic block polypeptoids were synthesized using surface initiated polymerization from a glass surface.[53] The height of the polymer brushes formed was characterized by atomic force microscopy, and the surface was characterized using contact angle measurements. Multiblock copolymers have also been synthesized on a polystyrene resin using ROP of *N*-substituted NCAs, a polymerization typically used in solution.[47] Up to five blocks of polymers with small side chains and low kg/mol molecular weights have been synthesized on a polystyrene resin, then cleaved and characterized with MALDI-TOF MS and ^{1}H-NMR. A strong Brønsted acid (HBF_4) was used to decrease the polydispersity ($Đ_M$ = 1.44) by slowing the polymerization. This synthesis is rapid and cost-efficient and is particularly promising due to the potential to be used in combination with submonomer peptoid synthesis or solid-phase peptide synthesis to create hybrid structures with unique bioconjugation capabilities and various applications.

2.2. Modified Primary Structure

Side chain diversity enables structural and functional control, but additional conformations and applications could be accessed by backbone-variants of the traditional α-peptoid. The most common variant of the *N*-substituted glycine peptoid backbone is the β-peptoid, or *N*-alkyl-β-alanine oligomer.[54] A variety of synthetic routes have been applied to the synthesis of these structures (**Figure 4**a), including multiple methods of solution phase polymerization. The first catalytic synthesis of poly-β-peptoids was reported by Hanton and coworkers.[55] This copolymerization of *N*-alkylaziridines and carbon monoxide was used to synthesize poly-β-peptoids with quantitative yields and controlled molecular weights (2 – 11 kg/mol with $Đ_M$ = 1.11 – 1.64). The reaction is catalyzed by $BnCOCo(CO)_4$, which is readily synthesized and purified with an extraction before polymerization. The polymers have been characterized by ^{1}H and ^{13}C-NMR in addition to IR and MALDI-TOF MS. This work was continued by Li Jia's group who investigated the mechanism of the polymerization with various catalysts.[56] Using the aforementioned technique, multiple side-products can form, including a lactam and polyamines instead of the amide based-polymer. To gain a more comprehensive understanding of the mechanism, in situ infrared spectroscopy was used to monitor chain growth over time. One of the catalysts, $CH_3C(O)Co(CO)_3P(o\text{-tolyl})_3$, allowed rapid dissociation of the $P(o\text{-tolyl})_3$ ligand, and the remaining cobalt complex efficiently performed the polymerization without catalyzing the formation of a lactam side-product. β-peptoids synthesized using cobalt-based catalysts were characterized using NMR and MALDI-TOF MS, and subsequently immobilized on gold as an anti-fouling material.[57] A similar technique involving the cobalt-catalyzed polymerization of *N*-alkylazetidine and carbon monoxide has been used to synthesize γ-peptoids, which contain one additional methylene in the backbone compared to the β-peptoid.[58,59] This synthesis does not have as high yield as those for β-peptoids due to competing reactions, and therefore the applications of these peptoid variants are rare.

Sequence-defined β-peptoids have also been synthesized using step-wise chemistry (Figure 4a). The first approach used a two-step monomer addition cycle involving acylation with

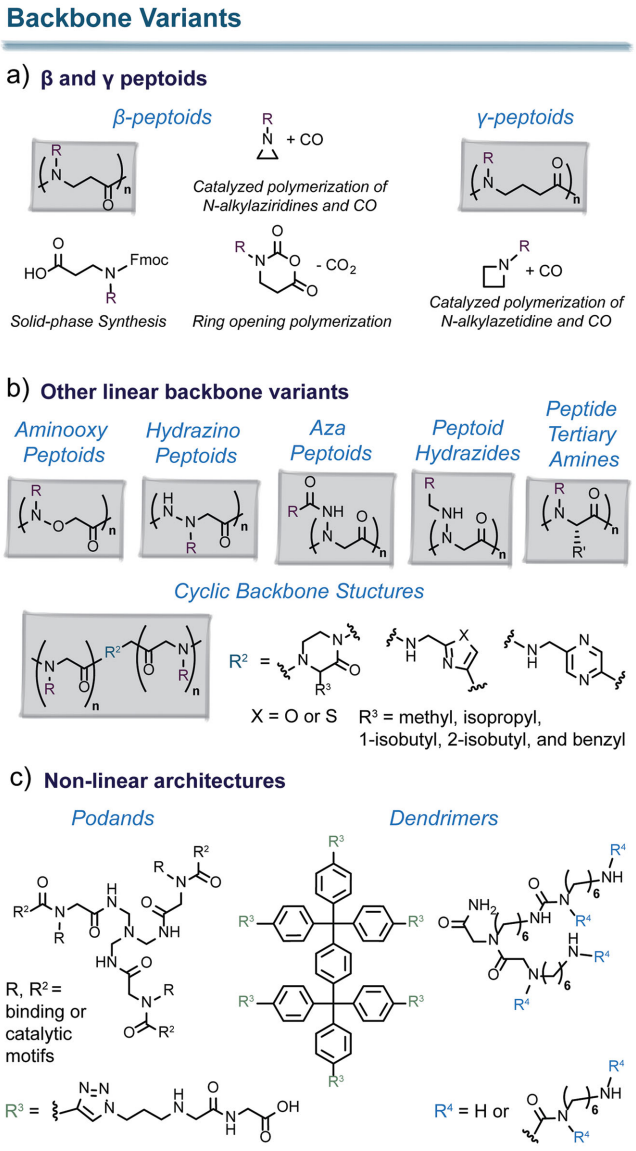

Figure 4. An outline of peptoid backbone variants. a) β-peptoid and γ-peptoid structures and synthesis techniques. b) Additional variations on the α-peptoid backbone structures. c) Branching peptoid-based structures. Various side chains were incorporated into the podand, and first, second, and third generation dendrimers were synthesized using the structures on the right.

an acrylic acid followed by a Michael addition with a primary amine.[60] Further work was done by Arvidsson et al. optimizing the synthesis and exploring Lewis acid catalysts.[61] They obtained the highest yields using Tentagel S PHB as a solid-support and a solvent system of water and tetrahydrofuran (THF). In this work, a nucleophilic submonomer synthesis similar to that used for α-peptoids was also evaluated and determined to be less efficient. Fmoc-protected monomers were also used to synthesize β-peptoids but led to poor yields.[62] A ring-opening polymerization was first investigated by Birkofer et al. with the polymerization of *N*-*p*-tolyl-β-alanine-*N*-carboxyanhydride.[63] This reaction has been more recently characterized establishing it's living character via kinetic analysis, and the polymerization has been used to synthesize block copolymers.[64] However, further characterization is still required as the molecular weights cannot be reliably predetermined.

The single methylene extension of β-peptoids is not the only backbone variant that has been explored. Aminooxy peptoids have been synthesized in both directions (C→N and N→C) using solution phase synthesis combining nitrobenzenesulfonamide-protected *N*-substituted aminooxyacetate *tert*-butyl esters (Figure 4b).[65] Several pentamers with hydrophobic side chains were synthesized using this method. Hydrazino azapeptoids have also been synthesized using a solution phase synthesis.[66] The Kodadek group has additionally worked towards the synthesis of several variants of the typical structure of an α-peptoid. To increase the conformational restraint and functionalization of the peptoid, peptoids with side chains on both the α-carbon (peptide-like) and nitrogen (peptoid-like) have been synthesized using a modification of typical submonomer synthesis.[67] All of these techniques add functional and structural diversity to the peptoid backbone; however, thus far they have been limited to low molecular weight compounds. Fortunately, the multifunctional submonomers pursued by the Kodadek group are compatible with the typical submonomer technique and could therefore be individually introduced into larger peptoid polymers.

The synthesis of azapeptoids has been achieved by the Kodadek group by using acyl hydrazides in place of the typical primary amine in the submonomer synthesis method.[68] The crystal structure of an acylated monomer indicated that acyl hydrazides tend to prefer *trans* amide bond geometries. Tetramer azapeptoids were synthesized to demonstrate that short structures could be prepared in high yields; however, this chemistry was found to undergo side-reactions under typical peptoid synthesis conditions as a result of intramolecular cyclizations. Further work indicated that these side reactions only occur when a methylene group precedes an aromatic group in the side chains of the azapeptoid.[69] To solve this problem, carbazates and semicarbazides were investigated as alternatives to the acyl hydrazides. These did not perform the undesired cyclization when incorporated with typical peptoid monomers. An octamer library combining typical peptoid monomers and those based on acyl hydrazides, carbazates, and semicarbazides was synthesized, demonstrating the compatibility of these reactions. There are many commercially available carbazates and semicarbazides, making this a promising technique for incorporating backbone diversity. Peptoid hydrazides, which have a similar structure to azapeptoids, have been synthesized using hydrazine as a monomer in the submonomer synthesis.[70] After the cleavage of the peptoid from the resin, modification with an aldehyde and reduction with sodium cyanoborohydride yielded a peptoid hydrazide backbone. This chemistry was used with akyl, aryl, and heterocyclic groups functionalizing the aldehyde.

The Kodadek group has also expanded the variety of peptoid backbone structures by incorporating cyclic molecules into the backbone of peptoids. This backbone design leads to unique structures resulting from the additional conformational constraints (Figure 4b). This conformational restraint is particularly advantageous as typical peptoid polymers are much more flexible than their corresponding peptides due to the loss of the chiral center.[71,72] The incorporation of heterocycles including oxazole, thiazole, and pyrazine structures into the middle of the backbone was optimized using microwave-assisted conditions.[73] These structures did not prevent sequencing with tandem-mass spectrometry of a combinatorial library. In additional work, 2-oxopiperazine was incorporated in the center of a peptoid backbone.[74] Unlike the heterocycles, which were added as monomers, the 2-oxopiperazine was formed on the solid-support by doing an intermolecular cyclization with an amine side chain and a C-terminal 2-chloroacetamide. The piperazine ring itself was functionalized with alkyl and benzyl side chains.

The primary structure of peptoids has additionally been modified by creating a variety of nanostructures using branching architectures. A one-pot synthesis was used to create peptide-peptoid podands built from tripodal skeletons.[75] Tri-acid, tri-amine, and tri-cyanate scaffolds were used to synthesize a variety of chimeric podands with functional groups including aromatic and heterocyclic rings as well as more complex structures such as steroids (Figure 4c). The modularity of the synthesis of these podands and cage structures allows for tunable and versatile structures. For instance, the environment formed by a tri-choline compound yields a unique exterior that changes hydrophobicity depending on the solvent microenvironment. These structures have potential applications the rapid identification of new catalysts and receptors.

Multiple groups have explored peptoids as the basis for dendrimers (Figure 4c). Bradley and coworkers used *N*-(6-aminohexyl)glycine as the monomer unit of their dendrimer, which was assembled on a solid-phase resin.[76] Microwave irradiation was used to accelerate the coupling reactions of the aminohexylglycine monomer. Three generations of dendrimers were synthesized; double couplings were required to ensure high yield in the second and third generation structures. Mass-spectrometry and HPLC were used to analyze the dendrimer products after ether precipitation, demonstrating an 85% yield for the final generation three dendrimer. These structures were evaluated as transfection agents and found to be non-toxic and able to transfect HEK293T cells. More recently, click chemistry has been used to assemble peptoid dendrimers on a hexaphenylxylylene (HPX) and tetraphenylmethane (TPM) core.[77] Rigid cores were constructed functionalized with alkyne or azide moieties, and peptoid arms were synthesized on solid phase with an N-terminal azide or alkyne-containing monomer and aryl or methoxyethyl side chains. The dendrimers were assembled using Cu-catalyzed

Adv. Mater. **2015**,
DOI: 10.1002/adma.201500275

click chemistry and washed with a solution of ethylenediaminetetraacetic acid. Dendrimers with the HPX core were found to be insoluble in organic solvents; however, dendrimers with the TPM core were soluble in polar solvents such as acetonitrile allowing HPLC purification. The dendrimers were characterized using electrospray ionization (ESI) MS and NMR diffusion-ordered spectroscopy (DOSY), allowing the calculation of the hydrodynamic radii of the compounds. All of these approaches to synthesizing branched peptoid structures have explored just a few of the potential structures available to *N*-substituted glycine oligomers; these structures could be uniquely useful as nanoarchitectures with more tunability and stability than their peptide counterparts.

2.3. Controlling the Secondary Structure

Although peptides primarily favor a *trans* amide bond, peptoid monomers can favor either the *cis* or *trans* orientation of the amide bond depending on local intramolecular interactions (**Figure 5**a). Therefore, many researchers have explored how to control the conformation of the amide bond by varying the size and electronic structure of the side chains and the interactions between the side chains and the backbone. One of the first investigations of the *cis* versus *trans* state was performed by Rabenstein et al.[72] They investigated the kinetics of the isomerization of the amide bond with butyl, benzyl, and methyl side chains in solution using NMR. All of the conformational isomers associated with structures containing one, two, and three amide bonds (representing two, four and eight conformations, respectively) were evaluated. The resonances of each isomer were assigned using total correlated spectroscopy (TOCSY) and rotating frame Overhauser effect spectroscopy (ROESY), and inversion-magnetization transfer NMR experiments were used to study the kinetics of exchange. Interestingly, it was observed that the isomerization rate was dependent on the location of the amide bond within the peptoid, and not necessarily just the side group. On average, 35% of the amides were in the *cis* conformation, which is slightly higher than the 10% typically observed with proline, the only proteinogenic *N*-substituted natural amino acid.[78] Additionally, the amide bond isomer tended to be affected by the orientation of neighboring amide bonds: when one amide bond favored a *trans* conformation, the neighboring amide bond demonstrated an increased preference for the *trans* conformation as well.

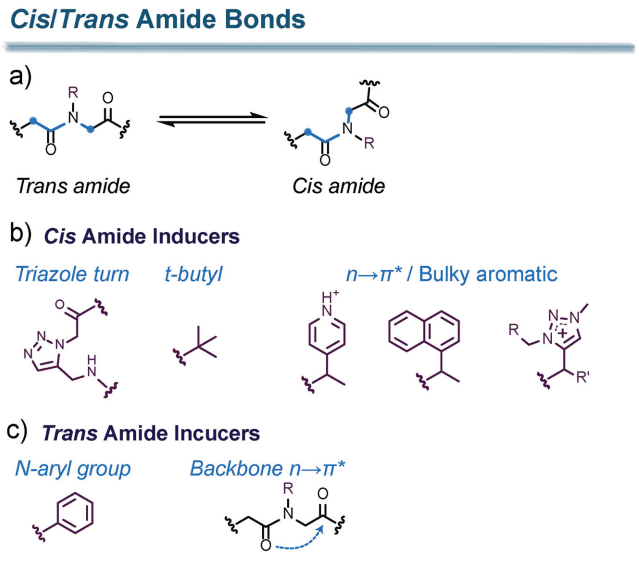

Figure 5. Structural features that induce *cis* vs. *trans* amide bonds. a) The equilibrium between the *cis* and *trans* amide bond is depicted with blue circles highlighting the difference in location of the α-carbons with respect to the plane of the amide bond. b) Turn and side chain moieties that will induce *cis* amide bonds. c) Structural features that lead to *trans* amide bonds.

The control of *cis* versus *trans* amide bond using side chain electronic effects has been investigated in detail. Loca et al. determined that the n→π^* interactions that have been characterized in polyproline sequences[79,80] can stabilize amide bond conformations in peptoids as well.[81,82] The n→π^* interaction between neighboring amides serves to stabilize the *trans* conformation (Figure 5c), while the n→π^* interaction between the amide and aromatic side chains or carbonyl-containing side chains serves to stabilize the *cis* conformation. The unusual *cis* conformation was observed in 89% of the amides using a positively charged α-chiral methylpyridine-containing side chain (Figure 5b). Solution phase studies were completed using ^{1}H-NMR and NOESY, and solid-state information was obtained from crystal structures. Gorske and coworkers continued to characterize the n→π^* stabilization and found evidence of a "bridged" interaction.[83] In this work over 90% of monomers with an α-chiral naphthyl or pyridine monomer formed a *cis* amide conformation. For the naphthyl compound, there is likely a steric component,[84] but generally computational analysis determined that for electron deficient aromatic side chains, a direct n→π^* interaction between the amide and the ring was the driving force stabilizing the *cis* amide bond. However, for rings with a higher electron density that contained an α-methyl group, a "bridged" interaction could contribute to the stabilization. For these cases, the σ^* orbital of the methyl group provides a bridge for the electron density from the carbonyl to contribute to the π-system of the aromatic ring.

Kirshenbaum and coworkers performed computational, NMR, and X-ray crystallography studies on *N*-aryl side chains to determine the conformational preferences of ten aniline substituents of varying size and electronic properties.[85] Quantum mechanical calculations on *N*-methylacetanilide-based monomers (the smallest aryl monomers examined) indicated a significant preference for the *trans* geometry (Figure 5c), and electron-donating groups tended to increase this preference with the reverse trend for electron-withdrawing groups. These results were confirmed by NMR studies; however, even an aniline with a fluorine substituent maintained a *trans*:*cis* ratio greater than 9:1.

Moieties that lead to an exclusive conformation of the amide bond are rare. Structures have been inserted to create turns in the middle of the peptoid backbone,[86] but only a few functional groups will lead to a single conformation. The Taillefumier group demonstrated that the *tert*-butyl side chain (Figure 5b) exerts a purely steric effect, forcing the *cis* conformation of the amide in both water and organic solvents as demonstrated by ^{1}H-NMR and NOE experiments where a *trans* conformation was

undetectable.[87] Of particular interest is the research displaying the conformational control provided by the triazole functional group in the side chains of α and β-peptoids.[88] In this work, α and β-peptoids were synthesized with propargylamine and later functionalized with Cu-catalyzed click chemistry. This chemistry has been used for post-synthesis functionalization in other reports;[30,77] however, this work demonstrated how the electron-deficient triazole, even with additional functionalization, can control the amide isomerism. A triazolium linkage led to greater than or equal to 89% of the population with *cis* conformations. With the neutral triazole, the *cis* conformation was still preferred, but to a lesser extent. These measurements were completed with NOESY, and the effect was investigated with a computational study of the potential energy surface. Their work attributes the stabilization of the *cis* amide to both the $n\rightarrow\pi^*$ interaction and an intramolecular H-bond between the triazole hydrogen and the neighboring carbonyl that is not involved in the $n\rightarrow\pi^*$ interaction.

Secondary structure in a peptoid polymer was first predicted with computational studies of peptoids with chiral side chains.[89] This analysis predicted asymmetric Ramachandran-like plots and therefore indicated the ability of side chains to induce a conformational preference for the amide bond. Barron and coworkers completed some of the initial analysis on forming peptoid helices using chiral aromatic side chains.[90] Since the peptoid structure lacks the amide hydrogen involved in stabilizing peptide helices, other stabilizing interactions are required. However, the incorporation of chiral aromatic monomers in excess of 50% of the total number of side chains was sufficient to confer helicity. Significantly, a chiral aromatic monomers at the C-terminus seemed to be required, though all of these requirements were relaxed with increasing length of the polymer. These helices were able to withstand temperatures up to 75 °C. A continuation of this work displayed the first crystal structure of a peptoid sequence (**Figure 6**a) which was a left-handed helix composed of chiral aliphatic side chains, demonstrating that aromatic monomers were not required for helix formation.[91] The crystal structure indicated an approximate pitch of 6.7 Å and three monomers per turn, results that are comparable to the polyproline type I helix. Both of these studies were important preliminary demonstrations of the capability of secondary structure within peptoid polymers. More recent work verified the significance of a chiral aromatic monomer at the C-terminus demonstrated by Barron et al. and indicated that in addition to the placement of a chiral monomer at the C-terminus, an α-chiral monomer at the second monomer from the *N*-terminus seems to also have a strong impact on the secondary structure of the peptoid polymer.[92] The presence of only one alpha chiral monomer in a heptameric peptoid placed in that position led to helical character measurable by circular dichroism (CD) spectroscopy. This work highlights the significance of the monomers, and their location in the primary sequence, in directing the peptoid secondary structure. Helices are a fundamental component of protein secondary structure, and therefore the development of peptoid helices is a stepping stone to assembling higher-order structures. Understanding how to control secondary structure formation is critical to the creation of functional peptoid polymer materials.

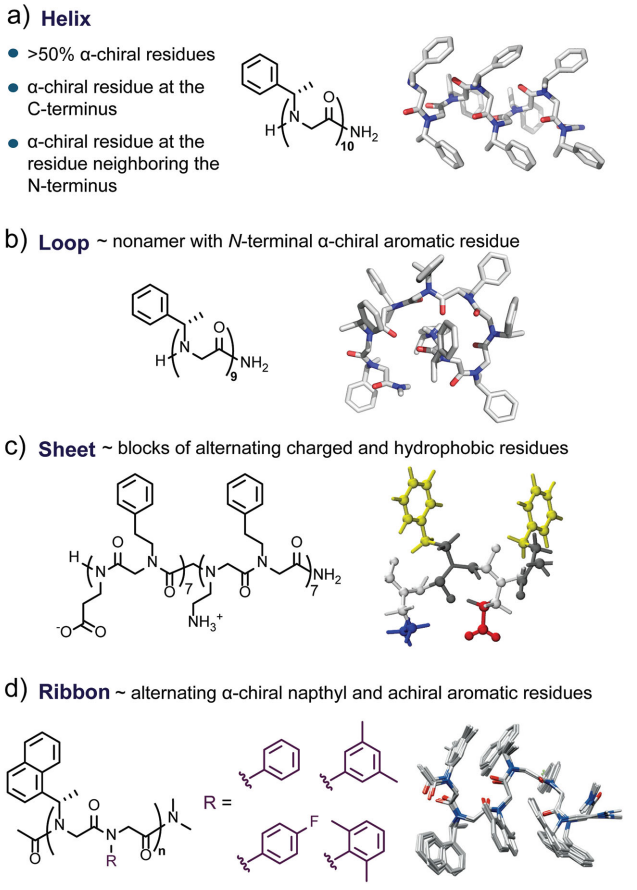

Figure 6. Using the primary sequence to control secondary structure. a) A list of primary structure characteristics that encourage the formation of a helix. The structure of a helix as generated using molecular mechanics is shown. b) A "threaded loop" secondary structure observed with peptoid nonamers. c) A sheet structure has been observed within peptoid nanosheets. The structure predicted with coarse-grained modeling is shown. d) The structure of a unique ribbon secondary structure is shown as an overlay of 10 low-energy structures, as determined by NMR spectroscopy. a) and b) Reproduced with permission.[96] Copyright 2009, American Chemical Society.

Research on peptoid helices has been expanded by incorporating functionalized chiral aromatic monomers. The synthesis of α-chiral phenyl monomers with *para*-substituted thiols, carboxylic acids, and amides was completed, and it was demonstrated that these monomers still directed helix-formation.[93] Peptoid sequences with a α-chiral pentafluorophenyl monomers were used to specifically probe helix-stabilizing interactions.[94] It was determined using NMR and CD that the hydrogen bonding of the monomer to neighboring heteroatoms was the most significant stabilizing force, and that there was no significant contribution from π-stacking. The placement of the α-chiral pentafluorophenyl monomer at the N-terminus of a nonamer predominantly led to the formation of a "threaded loop" that was previously identified by Radhakrishnan et al.[95] In a similar evaluation of a *para*-nitrophenyl α-chiral monomer, this monomer at the N-terminus also stabilized the formation

Adv. Mater. **2015**,
DOI: 10.1002/adma.201500275

of a threaded loop (Figure 6b).[96] However, the *ortho*-nitrophenyl had a destabilizing effect on the secondary structure of the polymer. Even this small chemical difference between the *ortho* and *para* nitro-groups has a significant impact on the folding of the peptoid.

The other canonical secondary structure for peptides, β-sheets, has been observed with peptoids as well. The Blackwell group has crystalized small peptoids with *N*-hydroxyamide peptoid dimers that appear to have β-sheet-like hydrogen bonding interactions between chains.[97] While these are very small structures, it is promising that the hydroxyl side chains could promote β-sheet-like structure in longer polymers. There has been evidence of β-sheet-like structure in longer polymers within the 2D-crystals, or nanosheets, designed by Zuckermann and coworkers (Figure 6c).[98] In these assemblies, the intetermolecular interactions are hydrophobic forces instead of the typical hydrogen bonding, but powder x-ray diffraction (XRD) has indicated a spacing of 4.5 Å between the polymers, indicating similar packing to peptide beta-sheets that have spacing of 4.7 Å due to hydrogen bonding.[99]

A unique secondary structure rationally designed by Blackwell and coworkers is the peptoid ribbon (Figure 6d).[100] This structure was obtained using alternating bulky α-chiral naphthyl monomers and achiral aromatic monomers, which led to alternating *cis* and *trans* orientations of the amide bonds. The ribbon itself had a helical conformation that was parallel to the backbone of the peptoid as characterized by X-ray crystallography, NMR, and CD. This conformation was maintained in protic and aprotic solvents and at different dilutions of the peptoid. This work and the previously described research characterizing the secondary structure of peptoid polymers has created a toolbox of moieties that allow for tunable structures while retaining functionality.

2.4. Bulk Properties

While precise sequence tunability enables some functionalities, an understanding of how to control the bulk properties of peptoid polymers is also important in the development of functional materials. Physical properties controlled by polymer composition include the crystallization and melting transitions. Side chains have been known to impact these properties for over 50 years, and therefore multiple groups have analyzed the impact of peptoid side chains on these properties. An evaluation of poly(*N*-ethylglycine) with differential scanning calorimetry (DSC) revealed a single glass transition temperature around 100 °C, indicating an amorphous structure.[101] This work also evaluated the melting behavior of peptoids with *N*- propyl, *N*-butyl, and *N*-pentyl side-chains finding that the melting temperatures decreased with the chain length and increased with increasing degrees of polymerization. The Zhang group built on this work by evaluating peptoid sequences synthesized by solution-phase polymerization and with linear alkyl side chains (**Figure 7**a).[102] Longer side chains led to two melting and crystallization temperatures and a loss of the glass transitions, likely due to the decrease in the volume of amorphous regions. The first melting temperature increases with the length of the side chains and was therefore attributed to side chain crystallization. The second melting temperature and associated enthalpies decreased with the increasing length of the side chains (for butyl and longer), and was thus attributed to main chain crystallization, which is hampered by increased ordering of the side chains. An investigation of branched side chains revealed they prevented packing of both the side chains and the main chain. Wide-angle X-ray diffraction indicated that heating followed by cooling slowly stimulated the crystallization of the peptoid polymers.

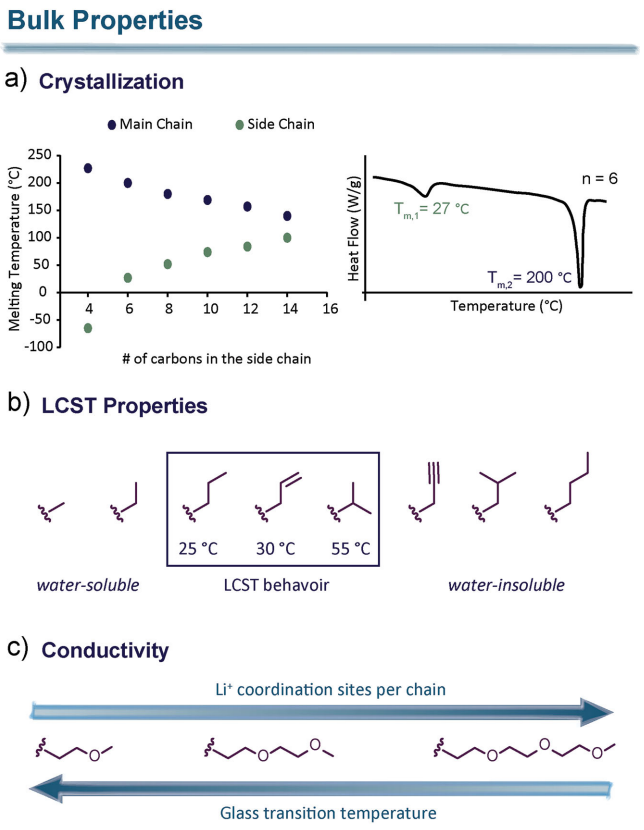

Figure 7. Characterized bulk properties of peptoid-based homopolymers. a) Melting transition temperatures of the main chain and side chain groups of alkyl homopolymers as measured with differential scanning calorimetry (DSC). An example DSC thermogram is shown for a hexyl homopolymer showing both melting transitions. b) Various peptoid polymers with small alkyl side chains were evaluated for thermoresponsive properties. Three were identified to have lower critical solution temperatures (LCSTs) in water within a physiological range. c) The conductivities of 20-mer polyethylene oxide mimetic polymer electrolytes were measured at a variety of lithium salt concentrations and temperatures to elucidate the structure-conductivity relationships of sequence-defined polymers. a) Reproduced with permission.[102] Copyright 2013, American Chemical Society.

To investigate the impact of introducing slight sequence variations on melting temperatures, sequence "defects" have been introduced to peptoid polymers.[103] In work by the Segalman and coworkers, several 15-mer peptoids were synthesized with the primary monomer having either isobutyl or 2-phenylethyl side chains with either two or four "defect" monomers (2-methoxyethyl, hexyl, or 3-phenylpropyl). The introduction of 2-methoxyethyl and hexyl defects into the isobutyl 15-mers

led to a slight change in packing as indicated by XRD, but a significant decrease in the melting temperature (up to 20 °C) with a continued decrease with increasing number of defects. Interestingly, the location of the defects also has an impact on the melting temperature and a slight impact on the packing. With precise control over the locations of the defects, it was determined that substitutions towards the center yielded the lowest enthalpies of melting, whereas substitutions near the termini yielded the highest enthalpies of melting. Surprisingly, the 3-phenylpropyl defects in the 2-phenethyl peptoid polymer completely prevented crystallization.

Similar classes of peptoid polymers have been evaluated for their thermoresponsive properties in water (Figure 7b). Copolymers of methyl and butyl monomers were discussed earlier,[52] but copolymers constructed from butyl- and ethyl-containing monomers were also evaluated by measuring the UV-vis transmittance over a range of temperatures.[104] The cloud point temperature could be tuned between 20–60 °C by varying the ratio of each monomer. Homopolymers with *n*-propyl, allyl, and isopropyl were also determined to have cloud point temperatures within that range (15–25 °C, 27–54 °C, and 47–58 °C respectively).[105] Due to semi-crystallinity of the propyl and allyl substituted samples, they had to be treated with methanol in order to solubilize them in water. Notably, propargyl substituted monomers resulted in a polymer that was insoluble in water. The precipitates formed by polymers of the propyl and allyl monomers above the cloud point formed a rose bud architecture as characterized by SEM. Polypeptoids with allyl side chains have been further studied to determine their thermoresponsive behavior and their behavior upon further photochemical modification with thiol containing moieties.[106]

Homopolymers of monomers bearing ethylene oxide-based substituents have been evaluated as polymer electrolytes for battery applications due to the high conducting capacity of poly(ethylene oxide) polymers containing dissolved lithium salts (Figure 7c).[107] The polymers were synthesized using step-wise solid-phase submonomer synthesis, allowing for the study of discrete polymer chains. Characterization was performed using small-angle X-ray scattering (SAXS), XRD, and DSC to determine that the structures are non-crystalline and have glass-transition temperatures, which vary based on the monomer. The transition temperature is increased with the introduction of lithium salts and increases linearly with concentration. The maximum conductivity was obtained with the polymer with the longest ethyleneoxy side chain, though this conductivity was dependent on the ion concentration. Increasing concentrations of lithium salts leads to increased conductivity; however, eventually the decreased chain mobility becomes a more significant effect and the conductivity starts decreasing with increased salt concentrations. The highest conductivity obtained (2.6×10^{-4} S/cm) was higher than those obtained with peptide-PEO mimetics. Interestingly, these block copolymers exhibited lamellar nanoscale phase-separated morphologies over a wide range of compositions.[108] It was also shown that the triethyleneoxy-containing peptoid block is amorphous as a homopolymer, but it will crystallize when appended to an *N*-decyl block (**Figure 8**a).[109] This enabled a direct comparison of the conductivities of an amorphous and crystalline phase of the same peptoid block.[110] The tunability of these structures will allow for future detailed analysis of modulation of ion conductivity by varying the primary structure.

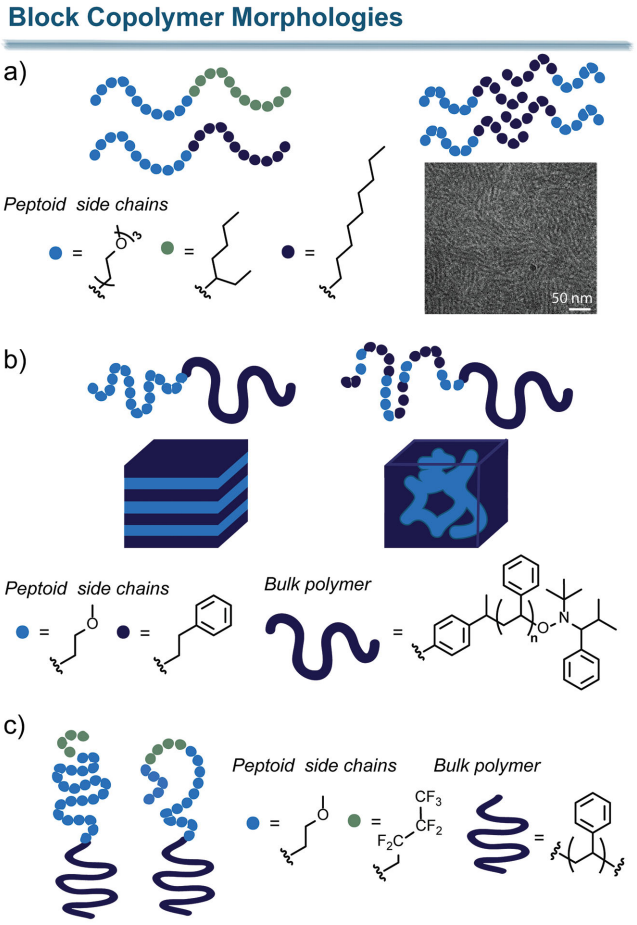

Figure 8. Investigations into the morphologies formed by block copolymers of peptoids (spheres) and polystyrene (solid lines). a) The morphologies of a completely peptoid-based block copolymer were evaluated with 38-mer diblocks. The polymer with the linear aliphatic substituents formed a crystalline block (TEM shown), while the shorter branched block formed amorphous structures conjugated to the same conducting block. b) Schematic of structures leading to lamellar and hexagonally packed morphologies based purely on the composition of the peptoid segment. Ratios between 4:6 and 6:4 styrene:methoxyethyl led to lamellar morphologies while 7:3 and 8:2 led to hexagonally packed structures. c) A block copolymer composed of three different monomers was used to evaluate how surface characteristics were affected by the placement of a fluorinated block.

Block copolymers and related materials are a natural research direction for peptoid polymers, but one that is only recently being extensively pursued. Polymerization,[111] stepwise synthesis,[108] and a combination of both[112] have been used to synthesize block-copolymers. Some of the first work on block-copolymers used peptoid polymers and polystyrene linked via click chemistry to study how to the peptoid composition affected the solid-state polymer assembly (Figure 8b).[112] An increase in the glass transition temperature was noted with increase in the ratio of aromatic monomers to 2-methoxyethyl monomers. Block copolymers of peptoids with a

Adv. Mater. **2015**,
DOI: 10.1002/adma.201500275

block of N-(2-methoxyethyl)glycine and a polystyrene block assembled into lamellar and hexagonally packed morphologies, as indicated by transmission electron microscopy (TEM) and SAXS analysis. As expected, composition ratios close to 1:1 form lamellar morphologies, and ratios closer to 7:3 or 8:2 form hexagonal morphologies. With the incorporation of N-2-phenylethyl side chains into the peptoid block, the phenyl monomers started mixing with the polystyrene phase, leading to decreased order in the assembled structure. This demonstrated that the modular sequence of the peptoid-block enables tuning of the segregation strength in the three-dimensional structure.

The ability to synthesize discrete molecules as blocks of multi-block copolymers has enabled detailed studies of surface exposed monomers in the assembly of a multi-block lamellar structure (Figure 8c).[113] These polymers were synthesized for antifouling applications, but provide interesting insight into the blurred borders between the lamellae of assembled block copolymers. Segalman and coworkers used a triblock copolymer, containing blocks of various lengths composed of benzyl, 2-methoxyethyl, and fluoroalkyl monomers, to explore the effect of the monomer ratios on the moieties exposed to the surface. X-ray absorption fine structure spectroscopy (NEXAFS) was used to characterize the exposed surface of the block copolymers. The surface segregation increases with the number of fluorinated monomers incorporated. Although lamellae are commonly described as having a defined boundary, there is typically significant mixing between the layers, and a block of five-fluorinated monomers increases this mixing such that peptoids up to 30-mer in size are unable to completely cover a surface from polystyrene exposure. Shifting the location of the fluorinated block to the middle of the peptoid structure decreases the thickness of the peptoid layer, increasing the amount of polystyrene displayed at the surface.

3. Surface Immobilized Polymers and Coatings

3.1. Antifouling and Antimicrobial Coatings

One important application of sequence specific polymers is to create functional coatings on materials. Maintaining the integrity of surfaces, from instruments as complicated as medical devices to surfaces as large as a ship's hull, has recently become a focus of ongoing research.[114] Coatings that can prevent the adhesion of proteins, bacteria, and marine microbes are incredibly important in maintaining the useful lifetime of materials. The Messersmith group began the application of polypeptoids as antifouling materials.[37] To achieve this, they focused on a class of peptoid polymers with short, hydrophilic side chains. They used a 25-mer of *N*-(2-methoxyethyl) glycine with a block of five monomers designed to mimic mussel adhesion peptides containing L-3,4-dihydroxyphenylalanine (DOPA) and basic primary amines. The 2-methoxyethyl monomers were chosen to enhance antifouling behavior – namely water solubility, charge neutrality, and the ability to accept hydrogen bonds. Over a period of five months, titanium-modified surfaces modified with these peptoid structures resisted cell adsorption as measured by fluorescence microscopy.

This work was recently expanded by a series of experimental and theoretical analyses. The same anchoring pentamer was used to immobilize varying lengths of 2-methoxyethyl peptoid polymers,[115] monodisperse polysarcosine sequences,[116] homopolymers of hydroxyl-containing monomers,[117] and heteropolymers with alternating charged monomers and 2-methyoxyethyl monomers.[118] Taking advantage of the tunability of the peptoid structures, zwitterionic heteropolymers of different lengths and different spacings between the charged monomers were synthesized and evaluated for antifouling capabilities. Slight differences were observed in the adherence of different cell types, which could be attributed to the aforementioned moieties. In another variation of this work, click chemistry was used to attach sugar units to the previously evaluated methoxyethyl peptoid polymer linked to the anchoring pentamer (**Figure 9**a).[119] These glycocalyx mimicking structures efficiently prevented a series of cells and proteins from adhering to a titanium surface, as demonstrated by fluorescence microscopy (Figure 9b). The results of molecular dynamics simulations indicate that sterics are likely the largest contributing factor to the antifouling behavior, in addition to water molecules bound to the terminal sugars. In a unique application of antifouling coatings, the methoxyethyl peptoid polymer and pentamer anchor were used to prevent protein adhesion on the imaging

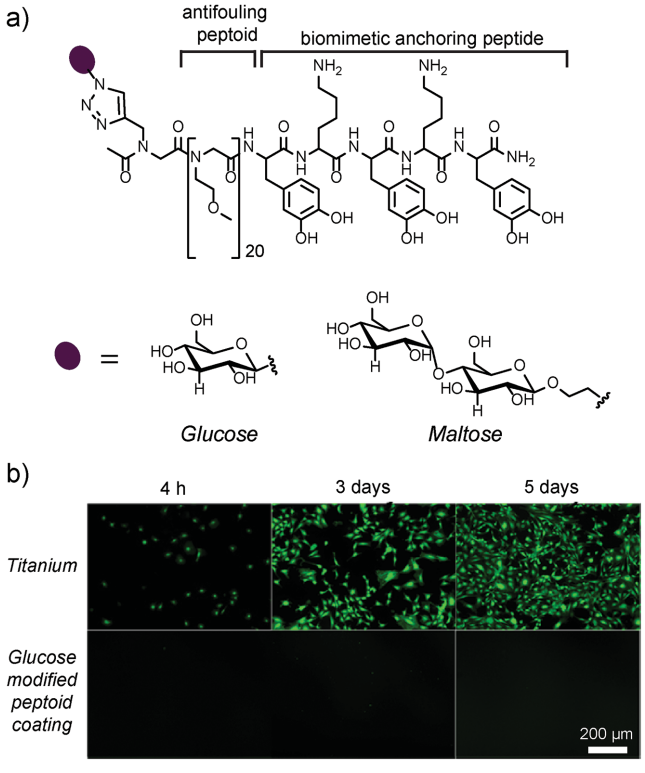

Figure 9. Chemical structures and an example application of antifouling peptoids. a) Peptoid structure terminating in a peptide mimetic of a DOPA-containing mussel inspired adhesion peptide linked using click chemistry to carbohydrates as a glycocalyx mimetic. b) Representative images of titanium surfaces with and without the peptoid-carbohydrate antifouling coating treated with fibroblasts demonstrate the ability of the glycocalyx mimic to prevent cell adhesion. Reproduced with permission.[119] Copyright 2013, American Chemical Society.

surface used for single-molecule microscopy.[120] Currently poly(ethylene glycol) methyl ether is used for this application, but this coating is labile to hydrolysis and can have unpredictable grafting densities. The peptoid polymer was demonstrated to be more effective at blocking non-specific protein interactions than the typical coating, demonstrating the practicality for future single molecule studies.

Peptoid polymers synthesized with living polymerizations have also been used as antifouling coatings. Poly(β-peptoids) were synthesized using cobalt catalyzed ring-opening polymerization and adhered to a gold surface using a terminal thiol.[57] Surface plasmon resonance spectroscopy was used to characterize the degree of protein adsorption. This was demonstrated to be an effective and synthetically scalable platform for coating surfaces. Ring-opening polymerization performed directly from the surface has also been applied and provides greater surface polymer densities.[53] An amine-silane was used to functionalize a glass surface, and block copolymers were synthesized directly from the amine moiety. Atomic force microscopy scans of the surface indicated a smooth surface with less than a 1 nm average roughness. Amphiphilic brushes were synthesized using two sequential surface initiated polymerizations and characterized using FTIR spectroscopy and X-ray photoelectron spectroscopy (XPS).

Another approach to anti-fouling is the immobilization of antimicrobial materials on the surface. This approach has been frequently applied with antimicrobial peptides.[121] The Barron group has recently published a number of studies mimicking antimicrobial peptides,[122,123] and the Winter group has applied combinatorial chemistry to this problem.[36,123] However, there is only one report of antimicrobial peptoids being immobilized on a surface.[124] In this work, the immobilized antimicrobial peptoids unfortunately did not prevent adhesion of bacteria to the surface, but the immobilized structures were determined to kill the bacteria that adhered. Although more bacterial adhesion was measured on a surface coated with polymers of methoxyethyl monomers and the antimicrobial peptoids than on a surface coated with the *N*-(2-methyoxyethyl)glycine polymers alone, the antimicrobial retained bactericidal effects. Future studies could involve a more detailed investigation of the ratios and lengths of the polymers, in addition to evaluating other antimicrobial structures.

3.2. Chromatography Supports

The ability to separate enantiomers of natural products and synthetic drugs is critical in a wide variety of biomedical applications. A variety of solid supports modified with ligands ranging from small molecules such as amino acids and cyclodextrins to full proteins have been developed to address this concern.[125] Their stability, ability to from secondary structures, and variety of available chiral submonomers make peptoids uniquely useful for this application. The Liang group has published a series of articles evaluating silica modified peptoid structures for these separations. In preliminary studies, polymers of *N*-(*S*)-1-phenylethyl)glycine monomers ranging from three to seven monomers in length were evaluated for their ability to isolate enantiomers of twelve different BINOL (1,1′-bi-2-naphthol) derivatives.[126] A dramatic increase in separation ability was seen with small increases in chain length. For BINOL itself, increasing the chain length significantly enhanced the separation ability, but this reached a maximum at 6 monomers, after which the separation ability started to decline. Methylation of the hydroxyls eliminated the separation ability, and placing bulky groups near the hydroxyls reduced the separation ability, confirming that hydrogen bonding between the substrates and the solid-phase serves as the primary interaction.

Future studies systematically varied the peptoid backbone to assess which other factors contributed to the ability to perform chiral separations. A series of peptoids built on a trimer of (*R*)-*N*-(1-phenylethyl)glycine evaluated the effect of varying the N-terminal moieties (**Figure 10**a). Various branched and unbranched alkyl chains, in addition to cyclic chiral and aromatic monomers, were evaluated. The chromatographic supports with achiral monomers at the N-terminus outperformed the polymers of (*R*)-*N*-(1-phenylethyl)glycine monomers of the same length. The authors hypothesized that this was due to the removal of unnecessary π-stacking interactions with the aromatic analytes. Additionally, the introduction of additional chiral structures to the N-terminus such as *N*′-phenyl-*L*-proline and *N*′-phenyl-*L*-leucine led to increased peak separation for specific analytes. Another study varied the chirality of the trimer (*R*)-*N*-(1-phenylethyl)glycine monomers and determined that heterogeneous chirality unexpectedly led to increased separation ability.[127]

The study of peptoid-based moieties for the separation of chiral products was expanded by creating a variety of branched structures. In recent work, a series of six branched structures

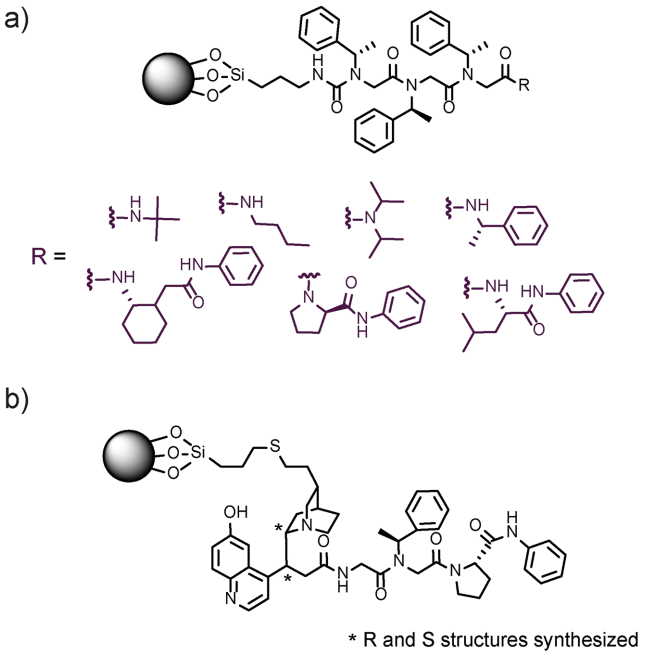

Figure 10. Peptoid structures analyzed for their performance in chiral separations. a) The effect of the N-terminal monomer of a trimer of (*R*)-*N*-(1-phenylethyl)glycine groups was investigated. b) The modification of branched peptoid structures with quinine and quinidine moieties was also evaluated.

Adv. Mater. **2015**,
DOI: 10.1002/adma.201500275

with six chiral centers was evaluated as chromatography supports; again the chirality was demonstrated to have a large effect on separation ability.[128] Heterogeneity in the chirality of neighboring structures led to increased separation ability, with one structure performing better than some commercial chiral chromatography columns. To increase the efficacy and analyte compatibility, the peptoid-base was expanded by modification with quinine and quinidine moieties, which have been demonstrated to be broadly applicable in chiral separations (Figure 10b).[129] These chromatography supports were demonstrated to outperform commercial quinolone-based supports for a variety of analytes. In some separations, the quinolone or quinidine moieties dominated the interactions with the analyte; however, for some of the separations hydrogen bonding and π-stacking with the peptoid played the most significant role in chiral recognition. The series of reports of peptoid-based chromatography supports demonstrate not only the applicability of peptoids for this application, but additionally how the sequence modularity can be used to create a library of supports tunable for the analytes at hand.

3.3. Materials Developed with Combinatorial Libraries

Combinatorial chemistry has played an integral part in industrial drug discovery in recent years, and thus a variety of techniques for spatially resolved immobilization of peptoids have been explored. One of the first was an adaption of the SPOT synthesis initially developed for peptides.[130,131] In this method, step-wise synthesis is performed on a cellulose membrane sheet where each individual reaction is spatially separated from its neighbor, leading to a library of thousands of compounds in a 2D array on the membrane. This technique was applied to the synthesis of a peptoid library in which 8000 peptoid hexamers were synthesized using the a modification of the submonomer method.[43] Due to the prevalence of free hydroxyl groups on the surface of the cellulose, bromoacetic acid 2,4-dinitrophenylester was used for the acylation step. The reliability of the synthesis technique was verified by cleaving individual peptoids and quantifying the purity with LC-MS (on average 44% purity), and the screening capabilities were evaluated by screening the library for antibody affinity.

A more common method of creating a spatially separated array of unique peptoids structures is to create microarrays on functionalized glass. The construction of microarrays from small molecules to proteins has been approached from a variety of perspectives, and there has been significant progress in their construction in recent years.[132,133] A microarray composed of a peptoid library was developed that created unique patterns for individual proteins, demonstrating the promise of peptoid libraries in biomedical detection devices.[134] For high yielding and pure peptoids, the synthesis was completed on a styrene-resin and then adhered to the maleimide-functionalized glass using a SpotArray 72 Microarray Printing System. Using microarrays of over 7500 compounds, they were able to create a "fingerprint" of hybridization unique to individual representative proteins. The protein was either fluorescently labeled or visualized with a fluorescent secondary antibody, and the patterns identified were both unique to the proteins of interest and reproducible (**Figure 11**a). This method could

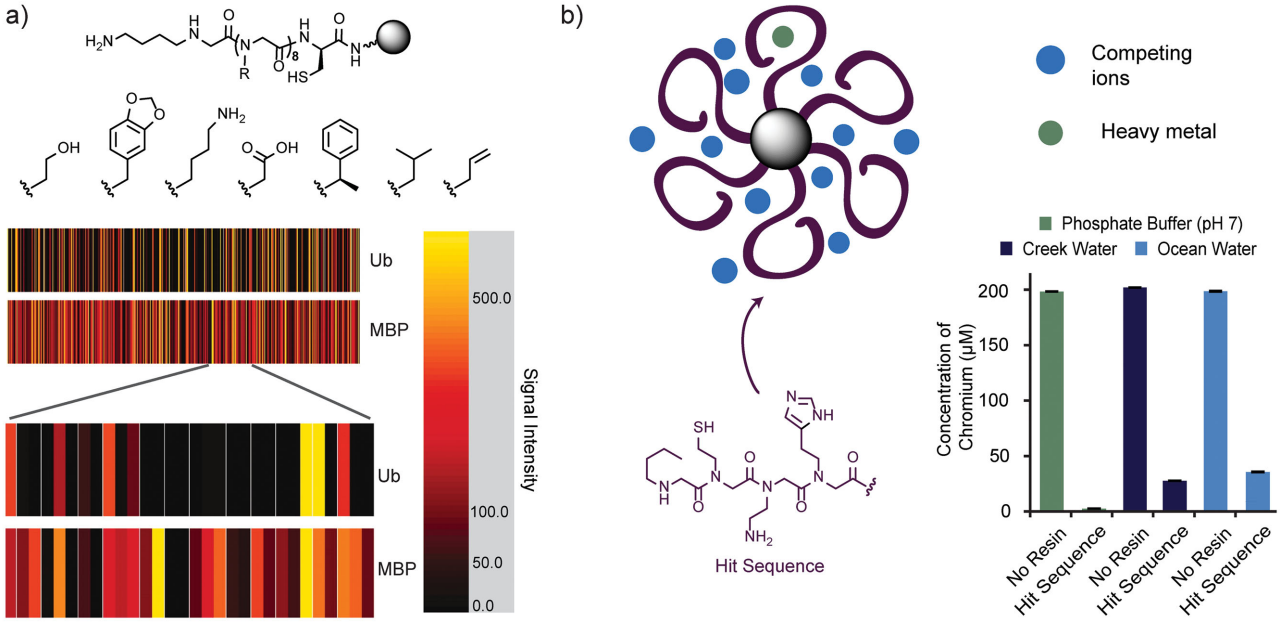

Figure 11. Application of combinatorial chemistry to the development of materials. a) Unique protein fingerprints. Peptoid microarrays displaying 7,680 distinct compounds (library schematic shown) were incubated with fluorescently labeled ubiquitin (Ub) and maltose binding protein (MBP). The fluorescence intensities were assigned to a color coding scheme as shown on the right, and depicted as a bar code for ease of visualization of binding. The expanded portion further illuminates the differences in the binding patterns. b) Metal binding peptoids identified using combinatorial chemistry were immobilized on polystyrene solid-supports (grey sphere). The ability of these structures to remove chromium(VI) selectively, a heavy metal contaminant, was evaluated by exposing the immobilized peptoids to various solutions with simulated chromium(VI) contamination. a) Reproduced with permission.[134] Copyright 2005, PNAS.

reliably detect less than 100 nM of a protein in the presence of *E. coli* cell lysate by subtracting background signal from the lysate proteins (and, when relevant, the secondary antibody). This detection limit is well below the binding affinities previously identified for peptoid-protein interactions, indicating the array itself is critical for the detection of low concentrations of proteins.

In variations of this work, the Kodadek group has also synthesized arrays of unique cyclic peptoids[135] and applied microarrays in the identification of high affinity ligands for proteins of interest.[44,136,137] The immobilization of cyclic peptoids was completed using maleimide-functionalized glass reacted with a cysteine adjacent to the peptoid sequence. The peptoid was cyclized following the on-bead deprotection of a carboxylic acid, which was then reacted with the N-terminus. After cleavage from the resin, the cysteine was robotically spotted onto the glass. A particularly interesting application of the microarrays in the development of diagnostics is the identification of fingerprint patterns for antibodies characteristic of Alzheimer's disease.[44] In this study, blood samples from patients were used to develop diagnostic readouts from a microarray of approximately 15 000 peptoid octamers.

Another unique application that demonstrates the applicability of combinatorial chemistry for materials applications is the identification of peptoid ligands. Some of the first work towards the identification of metal-binding peptoids was completed by Kirshenbaum and coworkers.[138] The binding of a pentamer and hexamer with terminal 8-hydroxy-2-quinoline methylamine monomers, and the affinities for Cu^{2+} and Co^{2+}, were characterized using titrations monitored with UV-vis and CD spectroscopy. The development of peptoid-based ligands has been continued with the development of cyclic peptoids which coordinate Na^{+} and Gd^{3+},[139,140] and combinatorial assays have been established to identify ligands with selective affinity for individual metal ions in a heterogeneous mixture.[38,141] X-ray fluorescence has been used as a screening technique for the identification of multiple metals coordinated to an individual resin-immobilized sequence.[141] As a proof-of-concept, this technique has been used to identify ligands for Ni^{2+} that can remove these ions from a buffered solution. Francis et al. used a colorimetric assay, based on previous work with peptide-based ligands,[142,143] to identify ligands which could coordinate toxic Cr^{6+} in multiple environments that simulated natural contaminated water (Figure 11b).[38] The ligands identified in the combinatorial screen were able to reduce the concentration of the contaminant to levels comparable to the EPA limit for drinking water. This work also includes structural variants and NMR characterization to illuminate interactions contributing to binding and selectivity. These studies demonstrate the capabilities of peptoids as metal ligands and highlight the use of combinatorial chemistry in identifying selective ligands. Though the applications of selective ligands are broad (therapeutics, imaging agents, sequestration, etc.) the factors contributing to selective binding are not well understood.[144] Due to the limited precedent for the rational design of selective ligands, these studies demonstrate the value of combinatorial chemistry for rapidly identifying new structures for unique materials properties including selective metal coordination.

4. Supramolecular Assemblies

4.1. Controlling the Crystallization of Materials

The crystallinity of biominerals like bone and abalone nacre is precisely controlled in nature by native biopolymers. The effort to reproduce this level of morphological control with inexpensive, well-defined synthetic materials has been approached both by studying the natural systems and by investigating the effects of synthetic polymers.[145] Recently, peptoid polymers have been applied to controlling the crystallization of calcite ($CaCO_3$),[146] and as antifreeze agents controlling ice crystallization.[147] Marine organisms naturally convert CO_2 to carbonate biominerals, and the nucleation of this mineralization has been demonstrated to be dependent on protein and peptide structures.[148,149] This is also an important topic of research as the sequestration of atmospheric CO_2 becomes increasingly important with the continued consumption of fossil fuels.

Peptoids have been rationally designed to mimic these mineralization proteins and have been demonstrated to control the growth of calcite.[146] Deyoreo, Zuckermann, and coworkers designed eight structures (examples shown in **Figure 12**a) based on the characteristics identified to impact the nucleation of calcite (e.g., the balance between hydrophobic and coordinating monomers). An analysis of the morphology of crystals grown in the presence of these peptoids revealed structures similar to those grown in the presence of the native proteins is shown in Figure 12b. Both the hydrophobic monomers and the number of acid monomers had an impact on the crystal formed, demonstrating significant tunability in the crystal morphology. Additionally, the AFM characterization of crystal growth indicated that a specific peptoid increased the rate of calcite crystal growth by a substantial 20-fold at nanomolar peptoid concentrations. Interestingly, at higher peptoid concentrations the degree of rate acceleration lessens, possibly due to surface binding. The authors suggest three possible mechanisms of rate enhancement: (1) coordination of calcium leads to an increased local concentration, (2) coordination decreases the energy barrier of desolvation for crystallization, and (3) the water layer is disrupted, decreasing the energetic cost of removing water from the crystal surface.

This work was continued recently with a series of 28 peptoid chains designed to continue the systematic evaluation of how simple sequence changes can impact the rate of calcite crystal growth and the final morphology.[150] In this study, the focus was on tuning the hydrophobicity of the structures by varying the number of hydrophobic monomers and their substituents. Hydrophobicity of the peptoid was seen to correlate with the reduced formation of {104} faces, but this could be modulated by the arrangement of the monomers in the sequence. Increasing electrostatic interactions between the anionic peptoid polymer and the calcite was seen to increase the formation of {104} faces as well, but the hydrophobicity was demonstrated to have a dominant effect. As the concentration of the peptoids was increased, the formation of {104} faces was decreased due to higher adsorption of the peptoid additives to the calcite surface. The ability to exert morphological effects on calcite growth was determined to be an effective method of preliminarily identifying structures that would accelerate the growth of calcite at

Adv. Mater. **2015**,
DOI: 10.1002/adma.201500275

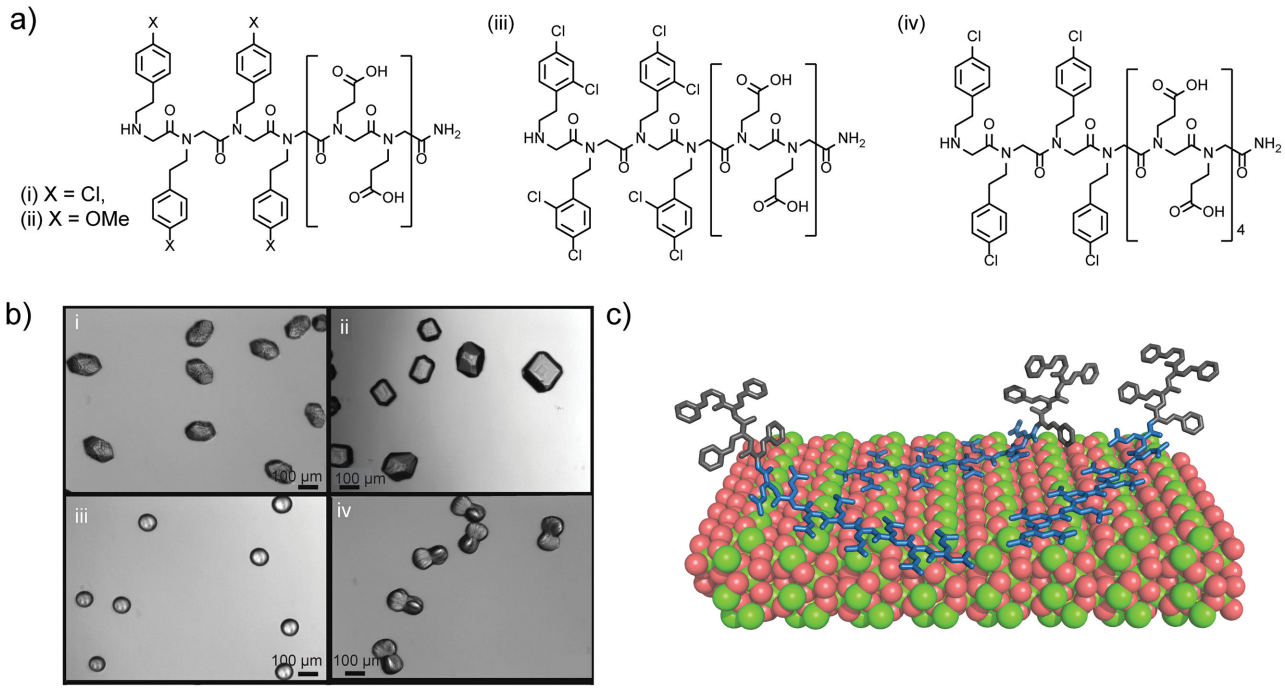

Figure 12. Studies of the peptoid modulated nucleation and growth of calcite have identified hydrophobicity and the fraction of carboxylic acids as characteristics affecting its growth. Eight structures were designed to evaluate these factors; a) some of these structures (i-iv) are shown. b) Crystal morphologies resulting from these four structures are shown. c) A model for the interaction between a peptoid structure and the calcite {104} face is shown, where the hydrophobic peptoid regions are represented in gray and the hydrophilic regions are in blue. b) Reproduced with permission.[146] Copyright 2011, American Chemical Society. c) Reproduced with permission.[150] Copyright 2014, Nature Publishing Group.

low peptoid concentrations. With additional AFM-based characterization of calcite-peptoid interactions, a model for peptoid interaction with the calcite was proposed (Figure 12c). The authors suggested that their work supports the third mechanistic proposal above: the adhered water is disrupted by peptoid-calcite interactions. The amphiphilic characteristics of the peptoids allow for diblock-like assembly, promoting growth as the carboxylic moieties reversibly interact with the surface of the crystal. The ability to mimic biomineralization is an exciting new application of peptoid polymers, given the significant amount of control obtained with peptoid polymers in calcite crystal growth.

In a similar application, peptoid polymers were investigated for their ability to control ice crystallization as antifreeze agents.[147] Despite ice being the most prevalent crystalline structure in nature, its crystallization is not fully understood. Antifreeze proteins in fish have evolved to control the crystallization of ice, artificially depressing the freezing point of water. These proteins have been extensively studied and mimicked with synthetic polymers; however, the details of the requisite interactions with ice are not completely understood.[151] The sequence control of peptoid polymers allows a specific investigation of the mechanisms of controlling ice morphologies and crystal growth. Homopolymers of lengths ranging from three to seven monomers of sarcosine, hydroxyl-containing monomers, and methoxyethyl monomers were synthesized, and their impact on ice morphology was evaluated with variable temperature video microscopy and compared to glycerol and oligoserine standards. Crystals grown in the presence of any of these additives were smaller than those grown in pure water, but the smaller tripeptoids led to the smallest crystals with the trimer of the hydroxyl-containing peptoid being the most effective. The rate of crystal growth was also impacted, with the trimer and hexamer peptoids displaying the slowest growth rates. Differential scanning calorimetry was used to evaluate the impact of the trimer additives on the melting temperature of the ice. The melting temperature was depressed for all of the samples with additives. The peptoid timers and serine trimer displayed a similar depression, with the exception of the sarcosine trimer which had a smaller effect. For each of these additives, the effect was determined to be more significant than that of colligative properties alone. By DSC, the hydroxyl-containing peptoid demonstrated the largest temperature change relative to the anticipated colligative effect. Given the successes of the hydroxyl-containing peptoid trimer in minimizing crystal growth and depressing the melting point, it would be interesting to continue to evaluate other monodisperse structures to further highlight the functionalities involved in controlling ice crystallization.

Preventing the crystallization of hydrates is also critical in the field of natural gas transportation.[152] The solid hydrate can form at low temperatures and high pressures, blocking transportation of natural gas. Typically poly(N-methacrylamide) derivatives are used for this application, but the amide backbone and hydrophobic side chains of peptoids are particularly useful for inhibiting the nucleation of hydrate crystals.[153] Jia and coworkers evaluated poly(*N*-alkyl-*β*-alanine) homopolymers and block copolymers as kinetic hydrate inhibitors by

evaluating the solubility at relevant pressures, the cloud points, and performance of the polymers in simulations of the real system. Polymers with longer akyl side chains performed better than shorter ones, and interestingly a random copolymer performed better than a block copolymer of the same composition. While peptoids have only begun to enter into the field of controlling crystallization, these studies demonstrate the promise of these highly tunable polymers for this application.

4.2. Solid-State Crystal Packing of Cyclic Peptoids

Since the first peptoid crystal structure was solved,[91] there have been a variety of interesting solid-state structures of peptoids that have been discovered. A recent review extensively covers the structures that have been identified for cyclic peptoids,[17] and here we highlight just a few interesting functional structures. In work by De Riccardis and coworkers, two of three synthesized cyclic peptoid structures formed a supramolecular assembly triggered by coordination of Na^+ (**Figure 13**a). This assembly is similar to metal organic frameworks (MOFs) and demonstrates the potential application of peptoids as tunable linkers for MOFs. The linkers control the assembly and final properties of MOFs;[154,155] thus, the tunability of peptoids is particularly applicable. Even with the sodium MOFs, slight differences between the peptoid structures evaluated (Figure 13a) lead to different solid-state properties. Of the three structures evaluated, the third structure does not crystallize, and the others lead to different coordination spheres despite containing the same coordinating moieties.

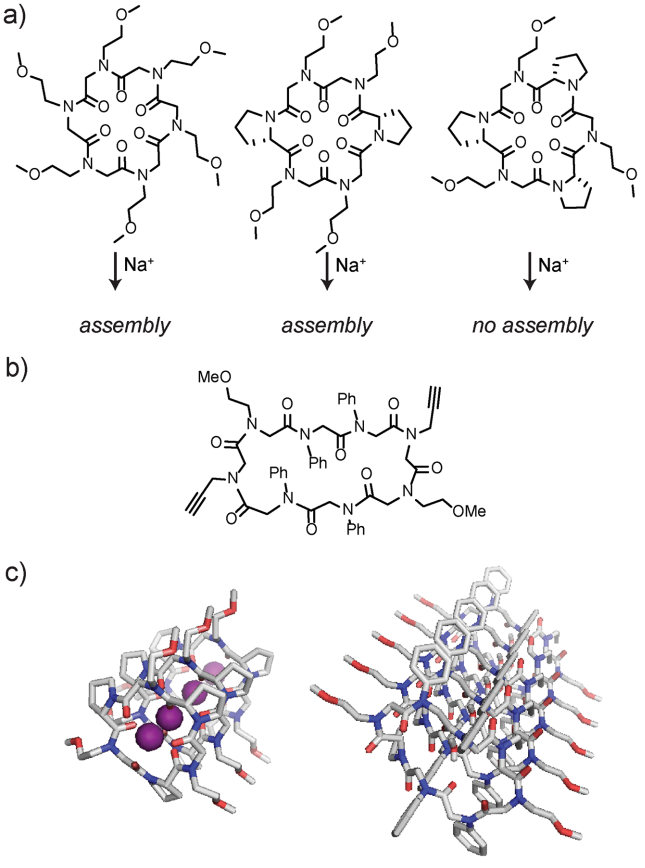

Figure 13. a) Structures of three hexameric cyclic peptoids, two of which form assemblies upon coordination of Na^+. b) A cyclic octamer that self-assembles into a nanotube without assistance from metal coordination. c) Crystal structures of the assembly of the middle structure in a) upon exposure to Na^+ (left) and of the cyclic octamer in b) (right).

Ordered solid-state structures have also been obtained without metal coordination. A cyclic octamer (Figure 13b) was designed with alternating *cis* and *trans* bonds to have predictable placement of the side chains.[156] The cyclic octamers self-assembled into a nanotube crystal structure with associated water molecules, demonstrating the ability to anticipate secondary structure (Figure 13c). The mole percent of water molecules was found to be variable depending on the crystallization environment, indicating possible diffusion of the water molecules through the nanotube crystal. Interestingly, the nanotubes were found to be stable up to temperatures of 300 °C, indicating the robustness of this structure. Given the applications that have been identified for peptide-based nanotubes, including in microelectronics and as biosensors,[157,158] it is likely that further research on the stable peptoid nanotubes will reveal additional applications in nanotechnology.

Only one cyclic nonamer (consisting of a repetitive (*R*)-*N*-(1-phenylethyl)glycine peptoid) has been crystallized, but what made the study of this nonamer particularly interesting was the comparison of its crystal structure to the structure predicted by molecular modeling.[159] We will discuss molecular modeling in more detail in a future section, but this highlights how the field is rapidly progressing towards predictable design of peptoid structures in the solid-state.

4.3. Solution-Phase Assembly of Defined Nanostructures

Moving beyond secondary structure, the development of tertiary and quaternary structural elements is the next step toward establishing protein-like control and functionality within peptoid-based synthetic materials. Supramolecular assembly is an expansive field with building blocks including small molecules, peptoids, polymers, and combinations thereof, and applications range from stimulus responsive materials to semiconducting nanofibers.[160–162] As sequence-defined polymers, peptoids could have an unprecedented diversity of conformations with the structural control necessary to take advantage of these. The design of supramolecular assemblies from peptoid polymers has just begun (examples shown in **Figure 14**a-c), but as more is learned about the properties of peptoids, this could be a rapidly expanding area of research.

One approach to the development of supramolecular peptoid assemblies has been to mimick naturally assembling peptides. Two peptoid structures have been synthesized that mimic self-aggregating amylin(20–29) that is associated with type II diabetes.[163] One of the peptoids is shown in Figure 14d and a TEM of the assembly is shown in Figure 14a. While this structure had some impact on the assembly of amylin(20–29), a peptoid with the reverse sequence inhibited the formation of peptide fibrils for at least four days. The self-assembling ability of these peptoid structures is particularly interesting because they

Adv. Mater. **2015**,
DOI: 10.1002/adma.201500275

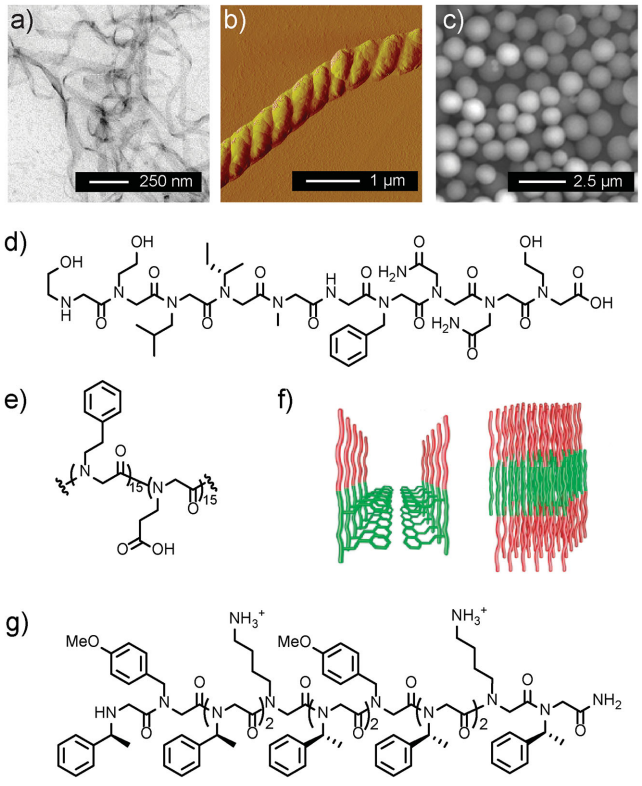

Figure 14. Self-assembled structures from amphiphilic peptoid polymers. a) TEM image of nanoribbons formed by the assembly of the peptoid structure in panel d. b) AFM image of a superhelix formed from the amphiphilic peptoid block copolymer shown in e). A model of the assembly is shown in panel f. c) SEM image of microspheres formed from structures in panel g. These images demonstrate the size diversity afforded by a simple rearrangement of monomers. a) Reproduced with permission.[163] Copyright 2007, Elsevier. b) and f) Reproduced with permission.[164] Copyright 2010, American Chemical Society. c) Reproduced with permission.[169] Copyright 2013, RSC Publishing.

have lost most of the hydrogen bonding pairs of the natural peptide. The assemblies are different than that of the natural peptide, and yet they still self-assemble.

One of the most unique structures that has assembled from peptoid polymers is a superhelix (Figure 14b) that was formed by an amphiphilic block copolymer.[164] Superhelices have been constructed from peptide-based copolymers before,[165] but this again demonstrates that the capabilities of peptoids are not limited by an achiral backbone. A 30-mer peptoid containing a block of 15 *N*-(2-phenylethyl)glycine moieties and a block of 15 *N*-(2-carboxyethyl)glycine moieties was synthesized on solid-phase (Figure 14e). After purification the structure was allowed to assemble in water buffered to pH 6.8. Within 24 hours, nanosheets assembled; after 4–7 days, they transitioned into superhelices (a model of the assembly is shown in Figure 14f). Once formed, the superhelices were incredibly stable in solution, lasting for months. The helices were characterized by SEM, TEM, AFM, and X-ray scattering, and were determined to have widths of approximately 625 nm and lengths varying from 2 to 40 μm. In an effort to relate the superhelix chirality to the molecular-scale peptoid chirality, chiral groups were introduced into the hydrophobic block. After alteration of one monomer had no impact on the structure, the entire block was replaced with chiral monomers. However, the superhelix chirality remained the same. This highly ordered structure holds promise for not only mimicking natural molecules that assemble into hierarchical helices, but additionally in gaining a more precise understanding of their self-assembly.

An important assembled structure in bioengineering is the hydrogel, which has applications ranging from sensors to tissue replacement materials.[166] Peptoid-based hydrogels are advantageous due to their biocompatibility and resistance to proteases. One approach to the construction of functional hydrogels was to combine a hydrophobic phenyl-based peptoid block with bioactive peptide trimers.[167] Four peptide sequences were chosen, and, in combination with the hydrophobic peptoid block, all of them formed hydrogels in phosphate buffered saline buffer (pH 7.4). The gels were characterized by rheometry and TEM to confirm gel formation and characterize the assembled structure. The oligomers with hydrophilic peptides assembled into sheet-like structures, and those with hydrophobic peptides assembled into networks of fibers. To confirm the biocompatibility of these gels, various cell lines were treated with the polymers in solution and in the gel and their rates of growth were evaluated. Another approach to the development of peptoid-based gels used a small library of peptoid dimers and a variety of solvents (not just water).[168] Optical micrographs of the gels formed show structures varying from uniform fibrous assemblies to heterogeneous sheets.

Another supramolecular morphology accessible to peptoid oligomers is microspheres (Figure 14c).[169,170] These have applications analogous to the previously described gel-like structures in drug delivery and sensing and similarly allow for a systematic evaluation of the molecular interactions leading to self-assembly. A panel of peptoid 12-mers with chiral helix-inducing, methoxybenzyl, acidic, and basic monomers was evaluated for self-assembly properties (example shown Figure 14g).[169] A comparison of two structures with very similar compositions showed that changing a single monomer made the difference between microsphere formation and no assembly at all. The microspheres that did assemble also varied ten-fold in size. This work was continued by investigating the properties required to coat these spheres uniformly on a glass or silicon substrate.[170] A microsphere coating could be advantageous for allowing ligand binding and for preventing surface fouling. The administration and drying techniques and solvent were seen to impact the microsphere coating process. Administration by dipping led to no microsphere coating, while administration of larger volumes followed by evaporation led to the formation of a well-distributed layer of microspheres.

A recently developed controllable class of peptoid supramolecular assemblies is two-dimensional crystals, or nanosheets (**Figure 15**).[98] The combination of two peptoid polymers, one that alternates hydrophobic and basic monomers and another that alternates hydrophobic and acidic monomers, leads to the formation of sheets with a thickness of 27 Å as indicated by analysis with powder XRD. The assembly takes place at micromolar concentrations in neutral aqueous solution. Most recent research on nanosheet-like structures has focused on graphene sheets, which may be prepared via exfoliation or organic synthesis, because of their potential applications in electronics.

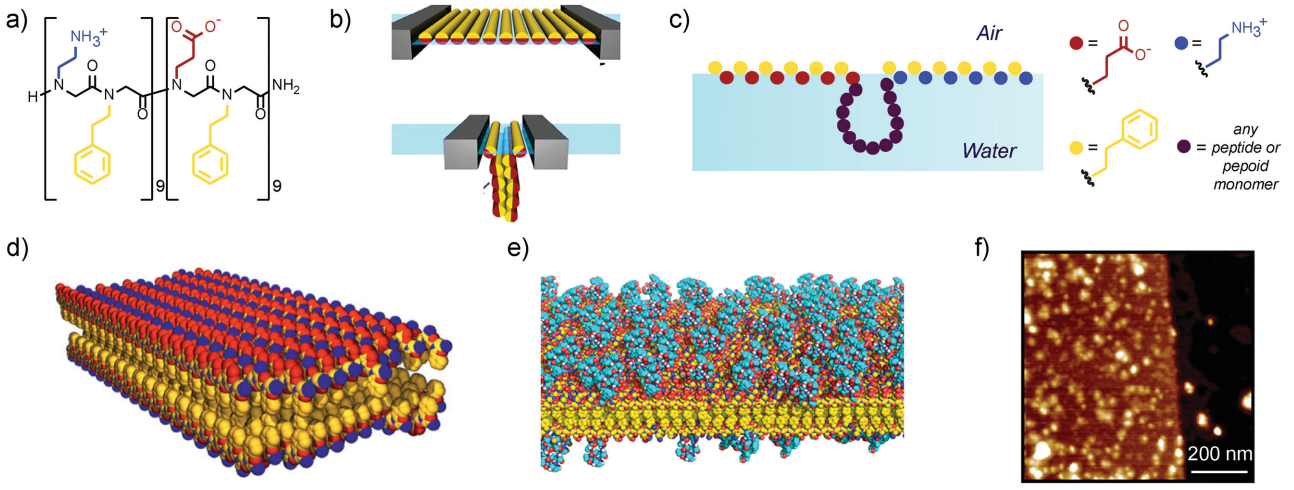

Figure 15. Peptoid nanosheet assembly. a) Structure of a peptoid polymer that leads to nanosheet assembly. b) Schematic of the assembly process due to monolayer formation at the air-water interface followed by compression. c) Schematic of a nanosheet with a loop region that projects from the surface. This loop region can be composed of any peptoid or peptide regions, including the functional region of anti-canine lymphoma IgG2 antibody. A 3D model of the assembled nanosheets is shown d) with and e) without a loop region. f) AFM images of peptoid nanosheets whose loop regions template the growth of gold nanoparticles after incubation with gold ions. b) Reproduced with permission.[171] Copyright 2011, American Chemical Society. d) Reproduced with permission.[98] Copyright 2010, Nature Publishing Group. e) and f) Reproduced with permission.[176] Copyright 2013, American Chemical Society.

However, two-dimensional crystalline materials also have potential applications in sensing, separations, device fabrication, and as biological tools. The work on peptoid nanosheets is particularly exciting as there are very few synthetic structures that self-assemble into planar sheets. To design these self-assembling materials rationally, the hydrophobic effect (a highly important driving force of protein folding) and electrostatic interactions were designed to hold together the assembled structure. The sequence programmability of the peptoids allowed for the synthesis of structures with various sequence patterns – $[(\text{charged})(\text{hydrophobic})_x]_y$, but only the alternating sequences self-assembled into nanosheets when mixed. To evaluate which forces are necessary for sheet formation, the charged monomers and then the hydrophobic monomers were replaced with a nonionic hydrophilic monomer. All of these substitutions prohibited sheet formation, confirming the necessity for both the hydrophobic and electrostatic interactions.

The peptoid nanosheets have been characterized with fluorescence microscopy (after the addition of Nile red), SEM, AFM, TEM, and X-ray diffraction. SEM images indicated that most sheets had lateral dimensions on the scale of tens of microns, and revealed sharp, flat edges of the sheets, suggesting that the peptoid oligomers align parallel to those edges. Aberration-corrected TEM was used to visualize the orientation of the peptoids, confirming their parallel orientation along the edge of the sheet. This again suggested a parallel chain packing geometry consisting of aligned, fully extended chains. An unusual mechanism of chain assembly was revealed after detailed studies indicated that a planar air-water interface was required for assembly. The observation that nanosheets only formed in samples that were shaken, not simply stirred, led to the hypothesis that these sheets were assembled via organization at the air-water interface into a monolayer, and then compression forced the collapse of the monolayer into a bilayer (Figure 15b,d).[171] A controlled, reproducible process of vial rocking was developed to allow systematically repeated monolayer adsorption and compression, which allowed for quantitation while avoiding abrasive shaking. The nanosheets formed with this mechanism were larger, but otherwise identical to those previously synthesized, as characterized by AFM and X-ray diffraction. The amount of peptoid converted into the nanosheet product was determined to increase linearly with the number of vial rotations, supporting the theory that monolayer compression at the air-water interface leads to bilayer formation. This process was additionally characterized via a Langmuir trough, which identified the pressure required to cause the collapse of the sheets (545.4 mN/m) and the time required to re-establish a surface monolayer of peptoids (450 sec). Interestingly, the sheets were demonstrated to be incredibly stable, and fluorescence recovery after photobleaching (FRAP) studies revealed that the individual peptoid chains are relatively immobile over 30 min.

Characterization and analysis of nanosheet formation was continued after determining that a single peptoid chain with both acidic and basic segments (Figure 15a) could lead to the assembly of nanosheets.[172] To further establish the requirements for nanosheet formation, self-assembly was evaluated at the interface between water and hydrophobic solvents.[173] In air-free environments, peptoid nanosheets were formed at the interface of water and pentane, hexane, or heptane, but not at the interface of water and more viscous solvents (decane and mineral oil) or aromatic solvents (benzene and toluene). Notably, nanosheets were formed at the water-carbon tetrachloride (CCl_4) interface, but they are much smaller. The authors indicate that this is likely due to the high affinity of CCl_4 for aromatic moieties. To investigate the monolayer density being formed at the CCl_4-water interface, the surface pressure was

Adv. Mater. **2015**,
DOI: 10.1002/adma.201500275

measured at both interfaces at various concentrations. The concentration required to saturate the surface monolayer (the maximum surface pressure) was higher for the air-water than the CCl_4-water interface, suggesting that there is some interaction between the peptoids and the carbon tetrachloride which disfavors the collapse into a bilayer. Characterization by X-ray diffraction and AFM confirmed that all other characteristics of the nanosheets were the same as those formed at the air-water interface. In this work, spectroscopy was used to characterize the sheet formation for the first time. Total internal reflection vibrational sum frequency spectroscopy was employed to characterize the monolayer formed at the CCl_4 water interface. Side chains were oriented perpendicular to the interface, and ion-pairs between the charged monomers were evident at high concentrations of peptoid. However, if the concentration was decreased and a less dense monolayer was formed, these electrostatic interactions were not observed. Similar spectra were observed for a peptoid polymer that lacked the acidic monomers. This sequence formed less tightly packed monolayers, likely due to electrostatic repulsion.

A detailed understanding of the nanosheet assembly process is critical for the future design of functional nanosheets. Analysis of the mechanism of peptoid packing revealed that the packing of the polymers occurs at the monolayer.[174] Grazing-incidence X-ray scattering was used to determine that the monolayer exists as a well-defined structure. A coarse-grained molecular model designed to predict the behavior of the backbone and side chains of the peptoids over a long time-scale was used to model the monomers at various concentrations.[175] The application of this modeling indicated that local ordering of side chain orientation is present in the monolayers at various surface densities of peptoid.[174] Increasing the temperature during nanosheet formation leads to an increased rate of assembly and a greater amount of nanosheets formed per vial rotation. This indicates that the formation of the monolayer is the rate-limiting step of nanosheet formation.

These compiled structural and mechanistic data are critical for the rational design of functional peptoid-based two-dimensional materials. Preliminary work has been directed toward the development of affinity reagents and substrates to template the growth of materials. The first report of functional peptoid nanosheets incorporated a streptavidin binding peptide at the terminus of the peptoid polymer and demonstrated that the assembled nanosheets could bind to a streptavidin-fluorophore conjugate.[98] Additional work by Zuckermann et al. has demonstrated the incorporation of enzyme substrates and gold-ligands that extend as loops from the plane of the nanosheet (Figure 15c,e).[176] Peptoid blocks in addition to functional peptides were inserted between blocks of alternating hydrophobic and charged monomers. The loops that formed in the monolayer were characterized using a Langmuir trough with X-ray reflectivity capabilities. This indicated that there was additional electron density below the typical peptoid monolayer that was attributed to the loop structure. Nanosheets with protease labile loops were incubated with a commercial protease cocktail, Pronase, and then the cleavage was confirmed by MALDI-TOF MS. Interestingly, however, there appeared to be no disassembly of the nanosheets as characterized by AFM. When nanosheets with the substrate for casein kinase II were incubated with the protein, phosphorylation was detected with a fluorescent antibody. As a final demonstration of the ability to incorporate functional loops, nanosheets containing a displayed gold nucleation peptide loop were mineralized in the presence of gold ion, and the resulting gold-plated nanosheets were characterized by AFM (Figure 15f). The capabilities of these nanosheets highlights the ability of peptoid-based materials to encode intentional protein-like architectural design and functional capacity into the primary sequence of the polymer.

5. Mimicking Natural Biological Constructs

5.1. Lipitoids and Surfactants

The non-viral delivery of nucleic acids into cells is critical for the development of stable, non-toxic, and inexpensive vectors for nucleic acid based pharmaceuticals.[177] With the recently discovered capabilities of the CRISPR/Cas9 system, there seem to be almost limitless applications of these RNA-guided nucleases.[178] Non-viral nucleic acid delivery is usually achieved by forming a complex with a cationic polymer of lipid. The development of lipitoids, or lipid-peptoid conjugates, was inspired by peptide-lipid hybrids, which have frequently been employed as cationic gene delivery agents[179] and drug delivery vehicles.[180] The first lipitoids were polymers of an amine-containing monomer attached to various lipids.[181] The step-wise synthesis of these structures allowed for a systematic evaluation of how the ratio of charge to hydrophobicity impacts the efficacy of the transfection. The peptoids that demonstrated the highest transfection activity also protected DNA from nucleases and contained a repeating trimer of a cationic monomer and two hydrophobic monomers. Interestingly, in a continuation of this work, the transfection efficiency could not be directly correlated with size, surface charge, structure (as characterized by CD), or affinity of the synthetic polymer for DNA (as measured by differential scanning calorimetry or ITC).[182]

Additionally, lipitoids have been used as an siRNA transfection agent, efficiently transfecting a variety of difficult cell lines, including primary human cells.[183] The lack of toxicity to immortalized cell lines was confirmed and efficient siRNA delivery was demonstrated by monitoring the target genes with Western Blots and real-time PCR. Additional SEM and DLS characterization was performed in follow-up work to characterize the particles formed from lipitoids and siRNA.[184] The size of the particles formed was found to vary depending the ionic strength of the environment and the ratio of lipitoid to siRNA.

Another approach to making functional amphiphilic peptoids has been extensively investigated by Barron and coworkers. Their work has focused on the mimicry of amphiphilic peptides and proteins using just the peptoid backbone.[185] Previous work has mimicked antimicrobial peptides by also varying simple arrangements of cationic and hydrophobic monomers.[186] The Barron group has also pioneered higher molecular weight analogs that mimic the helical and amphiphilic nature of lung surfactant protein C. The first peptoid developed for this purpose was a 22-mer containing a 14-mer of chiral aromatic monomers, two positively charged monomers, and a hydrophobic core. These structures served as a functional

surfactant without aggregating, demonstrating that a sequence-defined peptoid can mimic a 35-mer protein with additional protease resistance. This work was continued by investigating how adding alkyl chains to the N-terminus of this peptoid affected its activity.[187] These alkyl chains served as lipid anchors and increased dynamic film behavior by decreasing the compressibility, as measured by pulsating bubble surfactometry. Similar strategies have been applied to creating mimics of the larger protein, lung surfactant protein B,[188,189] and the addition of a lipid to the N-terminus of these molecules had a similar increased efficacy.[190] Interestingly, peptide-based mimics of lung surfactant protein B are more effective as dimers, so disulfide and triazole linkages of varying hydrophobicity were explored to dimerize the peptoid mimetic.[191] Dimerization by click chemistry surprisingly led to more surface activity than dimerization by disulfide formation, potentially due to the induction of a hairpin-like turn. The authors hypothesize based on these results that the conformational restraint within the native protein is important for its function. Additionally, the incorporation of achiral hydrophilic monomers into the linker, with 50% aliphatic monomers, led to activity improvement.

5.2. Protein-Like Polymers and Peptoid-Protein Hybrids

One of the first achievements towards mimicking protein structure and function with peptoid polymers was the development of a protein-like tertiary structure that experienced hydrophobic collapse, leading to the assembly of what was predicted to be a helix bundle.[192] In this work, a combinatorial approach was used to identify that monomers on the face of the helix were responsible for driving the assembly. Twelve hydrophobic monomers were introduced in four positions on the 15-mer peptoid to induce the hydrophobic collapse necessary for the formation of tertiary structure. The assembly of the identified helices into bundles was followed with circular dichroism (CD). This work was continued by linking together 15-mers through disulfide and oxime linkages to conjugate the helix bundles covalently.[193] Fluorophores were attached to each end of the peptoid polymer to allow for the detection of hydrophobic collapse via FRET quenching. Cooperative disassembly was observed upon titrations with various solvents, but the helical structure was unharmed, confirming that the FRET assay was an indicator of tertiary structure. Understanding the hydrophobic driving forces for the assembly of peptoid architectures is important for creating protein-like structures; however, this also fundamentally contributes to the understanding and prediction of protein folding itself.

The fundamental process of hydrophobic chain collapse, the coil-to-globule transition that is common to most protein folding pathways, has also been studied using specific peptoid sequence designs. Work by Zuckermann and coworkers investigated how the sequence of a peptoid polymer containing only one type of hydrophobic monomer and one type of polar monomer contributes to its hydrophobic interactions by synthesizing polymers with the same composition but different sequences (**Figure 16**a).[194] Because computer simulations required a 100-mer chain of defined sequence, two 50-mer peptoids were synthesized and dimerized using click chemistry.

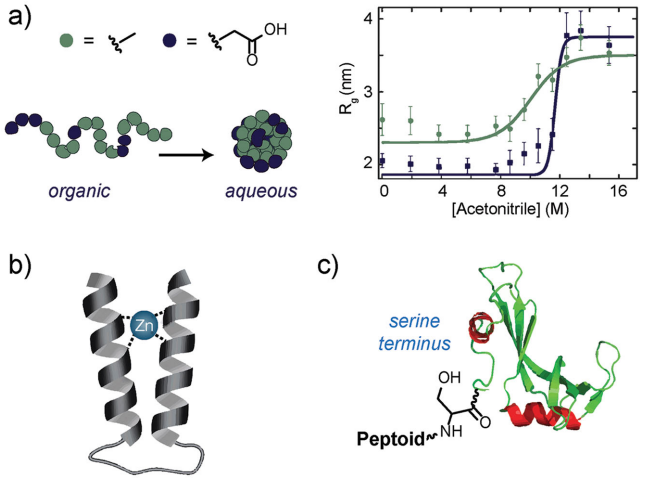

Figure 16. Protein-like structures synthesized with peptoid polymers. a) The hydrophobic collapse of polymers into globular structures in water and acetonitrile mixtures was evaluated for "protein-like" and "repeating" sequences with identical compositions but different monomer arrangements. This study indicated that the globular form of the "protein-like" structure was more stable in an organic solvent. b) A peptoid with helix bundle tertiary structure was stabilized with metal coordination. c) A peptoid was attached to ribonuclease S via an N-terminal serine. a) Reproduced with permission.[194] Copyright 2012, American Chemical Society. c) Reproduced with permission.[198] Copyright 2014, ACS.

One of the structures was designed to be "protein-like" and contained blocks of hydrophobic (*N*-methylglycine) and hydrophilic (*N*-(2-carboxyethyl)glycine) monomers designed using models described by Khokhlov and Khalatur,[195] while the other contained repeating blocks of [(*N*-methylglycine)$_4$-(*N*-(2-carboxyethyl)glycine)]. The stabilities of the assembled globule structures were evaluated by titration with acetonitrile as the unfolding was monitored using SAXS and DLS. The repeating sequence unfolded at lower concentrations of acetonitrile than the protein-like sequence, indicating decreased stability for the repeating structure. This was evidenced by a higher fluorescence signal with the protein-like polymer when probed with Nile red (an environmentally-sensitive dye), indicating a more intact globule. The free energy of the folding transition was calculated in addition to the dependence of that energy on the denaturant (m), both of which were larger for the protein-like sequence. Notably, a 100-mer peptoid polymer was synthesized in this work – one of the largest sequence-defined peptoid polymers that has been synthesized. This also demonstrates the ability to synthesize large polymers using post-synthetic conjugation. It additionally supports the previously mentioned models and demonstrates the utility of sequence controlled polymers in studying fundamental physical properties.

Another way to take on the properties of proteins is to mimic their function. In another report by Zuckermann et al., a peptoid helical bundle architecture was designed to mimic a zinc finger motif (Figure 16b).[196] Previously identified helical bundle designs[193] were modified with zinc-binding monomer units. The two helices were designed to contain two thirds α-chiral monomers to confer helicity and were built with repeating trimer sequences. The three monomers in the

Adv. Mater. **2015**,
DOI: 10.1002/adma.201500275

repeating unit were aromatic, acidic, and basic, and a turn sequence between the helices was composed of a Gly-Pro-Gly-Gly sequence or a repeating Gly unit. The zinc coordinating sites were based on an established motif, Cys_2His_2,[197] which was integrated into various sites in the polymer. Eleven peptoids were synthesized with the one of the two linkers and varying locations of the binding motif. A FRET-based assay was used to evaluate the proximity of the two helices in aqueous solution, and the proximity was further evaluated after titration with acetonitrile. Zinc-bound structures did not unfold upon the addition of acetonitrile, indicating the increased structural integrity of the metal-bound structures. This work includes one of few examples of a protein-like tertiary structure and highlights the use of combinatorial chemistry in the development of the precise molecular recognition necessary for higher-order structural control.

Recently, work by Kirshenbaum and coworkers has demonstrated that peptoids can be attached to proteins using a salicylaldehyde functionalized peptoid (Figure 16c).[198] Peptoids had previously been conjugated to small molecules and synthetic homopolymers;[112,113,199] however, this is the first combination of peptoid sequences and biological polymers. In this work, a ligation strategy developed for the reaction of *C*-terminal salicylaldehyde and an *N*-terminal serine/threonine[200] was applied to conjugate a peptoid and model proteins. The *C*-terminus of the peptoid was functionalized with the salicylaldehyde via an ester, and the model proteins were biosynthesized with the native *N*-terminal serine. The conjugation was completed in a 1:1 ratio of pyridine to acetic acid, which may not be compatible with all proteins of interest, and yielded up to 28% of the desired conjugate with a native amide bond between the peptoid and the protein. CD was applied to confirm that the peptoid did not impact the structure of the protein. In a similar application, individual peptoid monomers have been incorporated into the protein ribonuclease A.[201] These point mutations were incorporated using side-chain translocation mutagenesis. The successful incorporation of peptoid monomers could be used for applications ranging from well-controlled evaluations of the impact of individual monomers on secondary structure to engineering proteins with new functions. The combination of full peptoid sequences and the incorporation of an individual peptoid monomer could be used to combine the advantages of protein and peptoid structures.

5.3. Glycopeptoids

While the importance of glycosylation in biology has been well established, there has been a recent emergence of interest in building artificial glycan materials, including research focusing on glycan-conjugates in medicine,[202] glycopolymers used to study biological events,[203] and glyconanotechnology.[204,205] The interactions of these carbohydrate-based structures with cell receptors is critical for biological function and can therefore be extremely useful in the design of imaging probes and diagnostics. Given the complexity of natural glycans, this is a pertinent application of peptoids as sequence programmable polymers. The term "glycopepotids" was established by Roy et al. in the first description of carbohydrates incorporated into

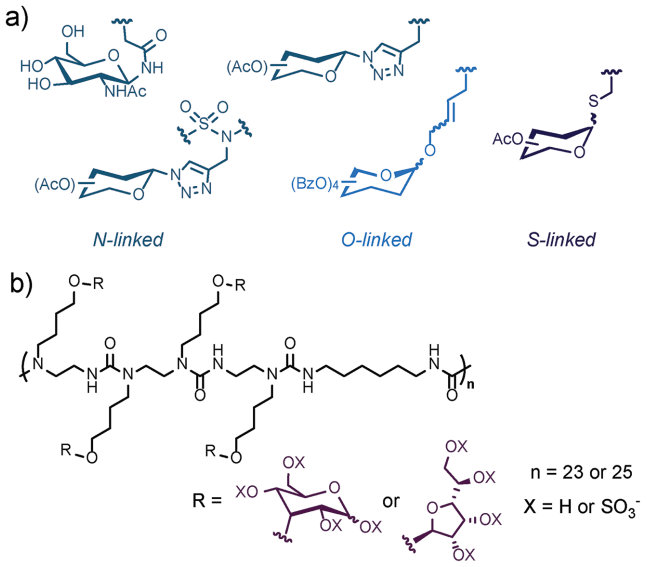

Figure 17. Glycopeptoids. a) Side chains with *N*, *O*, and *S*-linked carbohydrates. b) Polyurea glucose and mannose peptoid-based polymers. Sulfonated peptoid polymers mimic natural heparin for applications in biomaterials.

a peptoid side chain (**Figure 17**a).[206] The application of glycopeptoids as anti-fouling materials has been described above,[119] but that is only an introduction to the opportunities available. A recent review has summarized in detail progress towards the synthesis of glycopeptoids,[207] so here we will highlight some recent synthetic strategies and applications.

In the first synthesis of glycopeptoids by Roy et al., a submonomer-like synthesis with *N*-bromoacetyl derivatives and a glucose functionalized primary amine was applied to create an *N*-linked glycopeptoid.[206] A similar submonomer synthesis was applied in the synthesis of *S*-linked glycopeptoids by De Riccardis and coworkers (Figure 17a).[208] To clarify, "linked" does not refer to the linkage to the peptoid backbone, but instead to how the sugar is connected to the rest of the molecule; so, in the *S*-linked structure, the six-carbon sugar is connected to the peptoid through a thioether. While this is unlikely to affect the peptoid structure, it has a significant impact on the molecule's biocompatibility because this linkage is known to be more stable to hydrolysis than the *O*-linked analogues. Carbohydrate-containing primary amines were synthesized for incorporation into peptoid oligomers via submonomer synthesis. As is common with the functionalization of carbohydrates, the yield in the synthesis of the carbohydrate containing primary amines was low (averaging 50% for the six compounds synthesized). However, they could be synthesized with only a single purification step, and further steps proceeded with high yields. Some impurities were noted in a fully mannosylated hexamer, and it therefore seems unlikely that extended carbohydrate polymers could be synthesized with this method. However, this is a promising strategy for the incorporation of *S*-linked glycosylated regions within larger polymeric structures.

The natural *O*-linkage has been synthesized by Kwon and coworkers using on-bead using olefin cross metathesis, a reaction known to form carbon-carbon bonds efficiently

(Figure 17a).[209] In this work, a single sugar was incorporated; alkene moieties were incorporated as side-chains on the peptoid, and then the cross metathesis was used to attach an alkene-functionalized carbohydrate before cleavage from the resin. Combinations of butenyl-butenyl/pentenyl fragments gave the highest yields, and fortunately the chirality of the sugar and location of the alkene within the peptoid did not have a large impact on the yield of the reaction. Interestingly, the use of a PEGylated resin led to a higher yield for the cross metathesis reaction.

The natural glycosylation of *N*-linked glycoproteins could be critical to their function, yet this process is not fully understood. The synthesis of glycosylated substrates with this linkage could help understand the functionality of these sugars and provide a platform for the development of therapeutics. Various peptoids have been synthesized with reactive side-chain moieties for functionalization after the cleavage from a solid-phase resin, including *N*-alkylaminooxy[210] and propargyl[211] monomers. Using propargyl monomers and the established copper-catalyzed click chemistry to add carbohydrates (Figure 17a), recently Loganathan and coworkers synthesized "clickable" mimics of the natural linkage that is conserved in eukaryotic proteins [(D-GlcNac)-Asn-X-Ser/Thr].[212] In the original work by Roy et al., this sequence was mimicked with entirely peptoid monomers,[206] instead of the hybrid used in this work. Loganathan et al. suggest that the incorporation of small peptoid oligomers into a larger peptide could increase the structural diversity and stability of the polymer to proteolytic cleavage. Both α- and β-peptoid oligomers were synthesized with a variety of carbohydrate-based side-chains. Oligomers of these monomers with peptides were synthesized to mimic the natural linkage. These oligomers additionally included propargyl or azide moieties to enable further conjugation. This work was recently continued with the synthesis of peptoids with a sulfonamide backbone instead of the typical carboxyamide, and potential additional stabilization from hydrogen bonding with the sulfonamide oxygen was identified.[213] It is unknown what impact the presence of a small peptoid-based region will have on the stability or function of a larger polymer, but, as Loganathan and coworkers suggest, those studies are "just a click away."

Another approach to the synthesis of *N*-linked glycopolymers was completed by Ayres et al. (Figure 17b).[214] Instead of the typical α- or β-peptoid backbone, this peptoid structure was based on an *N*-alkyl urea backbone (a modification of the peptoid backbone mentioned above). The structures were synthesized to mimic heparin, a sulfonated glycopolymer that naturally serves as a coagulant and is commonly used in injectable gels.[215] Natural heparin has a few disadvantages, including significant heterogeneity and the necessity for obtaining it from animal tissues. Therefore, synthetic heparin could be valuable in various biomaterials applications.[214] Tetramers of glucose and mannose were synthesized by Ayres et al. in solution, and step-growth polymerization was used to incorporate these into hexamethylene diisocyanate polymers. These structures were deprotected, sulfonated, and characterized with FTIR and NMR spectroscopy. Additionally, a spin-cast film was characterized with contact angle measurements. Although no biological compatibility was evaluated, this work is exciting as one of few works to begin the characterization of polymer glycoconjugates.

6. Theoretical Modeling of Peptoid Architectures

A new tool in the development of peptoid polymers is theoretical modeling. It is quickly becoming one of the most useful methods for bridging the gap between synthetic and biological polymers. Due to the tremendous diversity of possible peptoid sequences, modeling is desperately needed to guide the rapid design and discovery of new peptoid-based materials, just as it has proved invaluable to the field of structural biology.[216] Research on peptoid modeling has been approached by adapting peptide force-fields (CHARMM),[217,218] integrating the noncanonical backbone into Rosetta,[219] and using various quantum-mechanical approaches. While there are well-established databases of tens of thousands of protein structures, there are few peptoids with known three-dimensional structures. However, even with the limited available information, models are beginning to be developed and applied, demonstrating the potential of this approach. Early insight into the folding landscape was provided by calculating Ramachandran plots for sarcosine, a model peptoid monomer.[13] Soon after this molecular mechanics predicted the formation of secondary structure by peptoid polymers.[89] A more detailed study characterizing the available peptoid backbone dihedral angles highlighted the impact of six different side chains of various sizes and chemical properties.[220] Density functional theory basis sets were used to evaluate the ability of the peptoid to rotate about each of the bonds in the backbone. As discussed in section 2, peptoids are capable of converting between *cis* and *trans* amide bonds and are less constrained to planarity of the amide bond than canonical peptides, making the isomerization of the amide bond an additional contributor to the number of available conformations. As expected, bulky side-chains can stabilize particular conformations of the peptoid backbones. All of the predicted bond angles were confirmed with the available crystal structures. While most of these structures are of small molecules, an understanding of peptoid topographies on this local scale can likely be extrapolated to larger structures.

The first demonstration of de novo structure prediction of a peptoid was demonstrated in 2012 when the structure of a cyclic nonamer was predicted and then confirmed by X-ray crystallography (**Figure 18**a).[159] A combination of Replica Exchange Molecular Dynamics (REMD) and quantum mechanical calculations was able to predict the structure of the nonamer to within 0.2 Å. This method was additionally used to predict the structure of trimers, but the nonamer is particularly interesting as it approaches the size of functional peptides. While a nonamer is still relatively small, this work was an important advance toward the current capabilities of protein modeling. The authors attribute differences between the predicted and experimental structures to solvent interactions, which were not included in the modeling algorithm. In another molecular dynamics approach, a new force field developed from first principles specifically for the peptoid backbone, called MFTOID, was derived based on the CHARMM simulation package.[221] This allows simulations both in a vacuum and in explicit water (the water was modeled as explicit molecules instead of as a continuous medium). This method was used to simulate a sarcosine dipeptoid and an *N*-(2-phenylethyl) glycine tripeptoid, and demonstrated the significance of solva-

Adv. Mater. **2015**,
DOI: 10.1002/adma.201500275

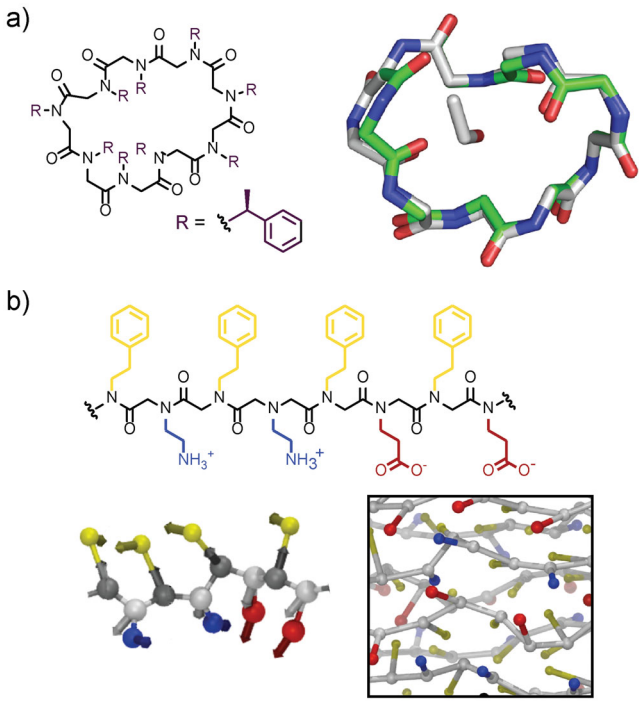

Figure 18. Theoretical modeling of peptoid structures. a) Nonamer structure with the experimental (gray) conformation as determined by X-ray crystallography is compared to a conformation predicted by molecular dynamics simulations (green). b) A segment of a peptoid polymer used for nanosheet formation represented as a chemical structure and a coarse-grained model. The nanosheet structure predicted by the model is also shown. a) Reproduced with permission.[159] Copyright 2012, PNAS. b) Reproduced with permission.[175] Copyright 2014, American Chemical Society.

tion in the structure of the peptoid backbone. In this report, the authors suggest that although no modeling of large peptoids had been completed, the small-scale evaluation of individual amide bonds in the peptide backbone has translated to larger proteins; therefore, as structural biology has grown rapidly with the established protein modeling capabilities, peptoid research should similarly be enabled by these computational procedures.

Despite the fact that the surge in peptoid modeling began recently, work towards modeling both large numbers of peptoids and high molecular weight structures is already underway. Some work to integrate experimental and in silico approaches has begun by using COSMOS-NMR that allows for three-dimensional modeling based on NMR data without the development of specific force fields.[222] An analysis of a cell-penetrating hexamer with two-dimensional NMR techniques allowed the amide bonds to be characterized as all *cis*, but did not allow for full characterization of the three-dimensional structure. However, with the aid of computational techniques, the structure was determined to be pseudo-helical. To enable entirely theoretical modeling of peptoid structures, recently the peptoid backbones have been integrated into the Rosetta platform typical used for protein modeling.[223] This was then used as a tool to create an in silico library of rotamers that represent the conformations available for over fifty side chains.[224]

One demonstration of theoretical modeling that is particularly applicable to materials applications was completed by Whitelam et al. who used coarse-grained sites to model peptoid polymers that assemble into nanosheets (Figure 18b).[175] Of particular interest in this work is the ability to model not only over longer length scales (which involve non-covalent interactions) but also over longer time scales, and with more polymer chains interacting. All of these features are necessary for understanding supramolecular assembly. To handle these increased demands, some sacrifices must be made in atomic representation – the described model is 10^4 times faster than a model that incorporates every atom. Typically in protein modeling, coarse-grained sites are treated as spherically symmetric. To compensate for this approximation, large numbers of these sites are used. In this work, a different approach was used, with only two sites per monomer fluctuating orientation parameters were incorporated for each of those sites. Due to the flexibility of the backbone compared to typical native biological structures, the models incorporated used independently fluctuating orientations (position and symmetry axes) to evaluate directionally dependent interactions. This model, termed MF-CG-TOID was used to model a 28-mer of alternating hydrophobic and charged monomers as a polymer in solution, as an assembled monolayer at the air-water interface, and as a nanosheet. Work is ongoing to analyze the dynamics of this process. Only with more experimentally determined structures can the accuracy of each of these modeling techniques truly be determined. However, with the diversity of approaches and successes thus far, the widespread modeling of peptoid polymers and assembled materials is certainly on the horizon.

7. Conclusion

As demonstrated in a growing number of examples, peptoid polymers offer wide-ranging opportunities for the construction of advanced biomimetic materials. By combining the features of high yielding synthetic procedures, substantial side chain diversity, improved processability, and improved stability toward enzymatic degradation, this new class of polymers is more practical for many applications than most natural biomolecules. In addition, their unique sequence programmability allows peptoid polymers to access sophisticated functions that require atomic-scale conformational control of the chain, or to achieve long range order that is not typically observed in traditional polymers. The efficient and modular step-wise synthesis of these polymers allows monomer-level control and fine-tuning of the polymer structure to precisely engineer polymeric materials for specific applications. Furthermore, it sets the stage for generating and screening vast combinatorial polymer libraries to facilitate the discovery of new materials with desired properties.

Additional opportunities arise as peptoids are combined with more traditional components such as surfaces, cofactors, nanoparticles, polymers, and biomolecules. The complex hybrid materials that result demonstrate advanced programmable functions, including gene delivery, surface antifouling, biomineralization, the detection of diagnostic analytes, and controlled macromolecular phase morphologies. The rapid expansion of

peptoid-based applications in recent years underscores their utility in providing ordered functional regions within bulk materials.

Looking ahead, an increasing number of studies are using design principles drawn from both structural biology and polymer science that can lead to predictable peptoid folding and self-assembly behavior. Protein-mimetic materials can now be made, for example, where each peptoid chain folds into a particular, well-defined nanostructure. This kind of structural control is bolstered by substantial recent progress on the computational front, which can now perform peptoid simulations over broad time and length scales. As peptoid-based materials find new applications, our fundamental understanding of the relationship between the chemical structure of the peptoid sequence and the functional properties of the assembled material will be elucidated. This will greatly improve our ability to engineer new peptoids with desired structural, functional, and interfacial properties, and will further close the gap between natural and synthetic polymers.

Acknowledgements

Work at the Molecular Foundry was supported by the Office of Science, Office of Basic Energy Sciences, of the U.S. Department of Energy under Contract No. DE-AC02–05CH11231. Additional funding for this work was generously provided by the NSF (CHE 1059083 and CHE1413666) and the Defense Threat Reduction Agency (DTRA10027-15875). A.S.K. was supported by a Philomathia Fellowship in Environmental Sciences.

Received: January 18, 2015
Revised: February 13, 2015
Published online:

[1] E. M. Nordwald, A. Garst, R. T. Gill, J. L. Kaar, *Curr. Opin. Biotechnol.* **2013**, *24*, 1017.
[2] T. L. Hendrickson, V. de Crécy-Lagard, P. Schimmel, *Annu. Rev. Biochem.* **2004**, *73*, 147.
[3] C. J. Noren, S. J. Anthony-Cahill, M. C. Griffith, P. G. Schultz, *Science* **1989**, *244*, 182.
[4] J. C. M. van Hest, K. L. Kiick, D. A. Tirrell, *J. Am. Chem. Soc.* **2000**, *122*, 1282.
[5] J.-F. Lutz, *Polym. Chem.* **2010**, *1*, 55.
[6] J.-F. Lutz, M. Ouchi, D. R. Liu, M. Sawamoto, *Science* **2013**, *341*, 1238149.
[7] C. J. Hawker, K. L. Wooley, *Science* **2005**, *309*, 1200.
[8] F. A. Leibfarth, K. M. Mattson, B. P. Fors, H. A. Collins, C. J. Hawker, *Angew. Chem. Int. Ed.* **2013**, *52*, 199.
[9] J. E. Poelma, B. P. Fors, G. F. Meyers, J. W. Kramer, C. J. Hawker, *Angew. Chem. Int. Ed.* **2013**, *52*, 6844.
[10] R. B. Merrifield, *J. Am. Chem. Soc.* **1963**, *85*, 2149.
[11] P. Cherkupally, S. Ramesh, B. G. de la Torre, T. Govender, H. G. Kruger, F. Albericio, *ACS Comb. Sci.* **2014**, *16*, 579.
[12] J. Sun, R. N. Zuckermann, *ACS Nano* **2013**, *7*, 4715.
[13] R. J. Simon, R. S. Kania, R. N. Zuckermann, V. D. Huebner, D. A. Jewell, S. Banville, S. Ng, L. Wang, S. Rosenberg, C. K. Marlowe, *Proc. Natl. Acad. Sci. U. S. A.* **1992**, *89*, 9367.
[14] R. Potyrailo, K. Rajan, K. Stoewe, I. Takeuchi, B. Chisholm, H. Lam, *ACS Comb. Sci.* **2011**, *13*, 579.
[15] B. Yoo, K. Kirshenbaum, *Curr. Opin. Chem. Biol.* **2008**, *12*, 714.
[16] S. A. Fowler, H. E. Blackwell, *Org. Biomol. Chem.* **2009**, *7*, 1508.
[17] C. Tedesco, L. Erra, I. Izzo, F. De Riccardis, *Cryst. Eng. Comm.* **2014**, *16*, 3667.
[18] D. Zhang, S. H. Lahasky, L. Guo, C.-U. Lee, M. Lavan, *Macromolecules* **2012**, *45*, 5833.
[19] A. M. Rosales, R. A. Segalman, R. N. Zuckermann, *Soft Matter* **2013**, *9*, 8400.
[20] N. Gangloff, R. Luxenhofer, *Adv. Polym. Sci.* **2013**, *262*, 389.
[21] A. E. Barron, R. N. Zuckermann, *Curr. Opin. Chem. Biol.* **1999**, *3*, 681.
[22] R. Luxenhofer, C. Fetsch, A. Grossmann, *J. Polym. Sci., Part A: Polym. Chem.* **2013**, *51*, 2731.
[23] K. H. A. Lau, *Biomater. Sci.* **2014**, *2*, 627.
[24] R. N. Zuckermann, J. M. Kerr, S. B. H. Kent, W. H. Moos, *J. Am. Chem. Soc.* **1992**, *114*, 10646.
[25] T. S. Burkoth, A. T. Fafarman, D. H. Charych, M. D. Connolly, R. N. Zuckermann, *J. Am. Chem. Soc.* **2003**, *125*, 8841.
[26] A. S. Culf, R. J. Ouellette, *Molecules* **2010**, *15*, 5282.
[27] N. H. Shah, K. Kirshenbaum, *Org. Biomol. Chem.* **2008**, *6*, 2516.
[28] C. W. Wu, T. J. Sanborn, K. Huang, R. N. Zuckermann, A. E. Barron, *J. Am. Chem. Soc.* **2001**, *123*, 6778.
[29] T. Horn, B.-C. Lee, K. A. Dill, R. N. Zuckermann, *Bioconj. Chem.* **2004**, *15*, 428.
[30] J. M. Holub, H. Jang, K. Kirshenbaum, *Org. Biomol. Chem.* **2006**, *4*, 1497.
[31] T. Kawakami, H. Murakami, H. Suga, *J. Am. Chem. Soc.* **2008**, *130*, 16861.
[32] Y. Shimizu, A. Inoue, Y. Tomari, T. Suzuki, T. Yokogawa, K. Nishikawa, T. Ueda, *Nat. Biotechnol.* **2001**, *19*, 751.
[33] Y. Goto, T. Katoh, H. Suga, *Nat. Protoc.* **2011**, *6*, 779.
[34] L. N. Monsalve, G. Petroselli, R. Erra-Ballsells, A. Vázquez, A. Baldessari, *Polym. Int.* **2014**, *63*, 1523.
[35] R. N. Zuckermann, *Pept. Sci.* **2011**, *96*, 545.
[36] S. Ng, B. Goodson, A. Ehrhardt, W. H. Moos, M. Siani, J. Winter, *Bioorg. Med. Chem.* **1999**, *7*, 1781.
[37] A. R. Statz, R. J. Meagher, A. E. Barron, P. B. Messersmith, *J. Am. Chem. Soc.* **2005**, *127*, 7972.
[38] A. S. Knight, E. Y. Zhou, J. G. Pelton, M. B. Francis, *J. Am. Chem. Soc.* **2013**, *135*, 17488.
[39] D. G. Udugamasooriya, S. P. Dineen, R. A. Brekken, T. Kodadek, *J. Am. Chem. Soc.* **2008**, *130*, 5744.
[40] L. S. Simpson, T. Kodadek, *Tetrahedron Lett.* **2012**, *53*, 2341.
[41] T. M. Doran, Y. Gao, K. Mendes, S. Dean, S. Simanski, T. Kodadek, *ACS Comb. Sci.* **2014**, *16*, 259.
[42] S. Li, D. Bowerman, N. Marthandan, S. Klyza, K. J. Luebke, H. R. Garner, T. Kodadek, *J. Am. Chem. Soc.* **2004**, *126*, 4088.
[43] N. Heine, T. Ast, J. Schneider-Mergener, U. Reineke, L. Germeroth, H. Wenschuh, *Tetrahedron* **2003**, *59*, 9919.
[44] M. M. Reddy, R. Wilson, J. Wilson, S. Connell, A. Gocke, L. Hynan, D. German, T. Kodadek, *Cell* **2011**, *144*, 132.
[45] F. Sigmund, F. Wessely, *Hoppe-Seyler's Z. Physiol. Chem.* **1926**, *157*, 91.
[46] C. Fetsch, R. Luxenhofer, *Macromol. Rapid Comm.* **2012**, *33*, 1708.
[47] N. Gangloff, C. Fetsch, R. Luxenhofer, *Macromol. Rapid Comm.* **2013**, *34*, 997.
[48] C. Fetsch, A. Grossmann, L. Holz, J. F. Nawroth, R. Luxenhofer, *Macromolecules* **2011**, *44*, 6746.
[49] L. Guo, S. H. Lahasky, K. Ghale, D. Zhang, *J. Am. Chem. Soc.* **2012**, *134*, 9163.
[50] C.-U. Lee, T. P. Smart, L. Guo, T. H. Epps 3rd, D. Zhang, *Macromolecules* **2011**, *44*, 9574.
[51] X. Tao, C. Deng, J. Ling, *Macromol. Rapid Comm.* **2014**, *35*, 875.
[52] X. Tao, Y. Deng, Z. Shen, J. Ling, *Macromolecules* **2014**, *47*, 6173.
[53] M. Schneider, C. Fetsch, I. Amin, R. Jordan, R. Luxenhofer, *Langmuir* **2013**, *29*, 6983.

[54] C. A. Olsen, *Biopolymers* **2011**, *96*, 561.
[55] L. Jia, H. Sun, J. T. Shay, A. M. Allgeier, S. D. Hanton, *J. Am. Chem. Soc.* **2002**, *124*, 7282.
[56] D. J. Darensbourg, A. L. Phelps, N. Le Gall, L. Jia, *J. Am. Chem. Soc.* **2004**, *126*, 13808.
[57] S. Lin, B. Zhang, M. J. Skoumal, B. Ramunno, X. Li, C. Wesdemiotis, L. Liu, L. Jia, *Biomacromolecules* **2011**, *12*, 2573.
[58] J. Chai, G. Liu, K. Chaicharoen, C. Wesdemiotis, L. Jia, *Macromolecules* **2008**, *41*, 8980.
[59] G. Liu, L. Jia, *Angew. Chem. Int. Ed.* **2006**, *45*, 129.
[60] B. C. Hamper, S. A. Kolodziej, A. M. Scates, R. G. Smith, E. Cortez, *J. Org. Chem.* **1998**, *63*, 708.
[61] A. S. Norgren, S. Zhang, P. I. Arvidsson, *Org. Lett.* **2006**, *8*, 4533.
[62] C. A. Olsen, M. Lambert, M. Witt, H. Franzyk, J. W. Jaroszewski, *Amino Acids* **2008**, *34*, 465.
[63] L. Birkofer, H. Kachel, *Naturwissenschaften* **1954**, *41*, 576.
[64] A. Grossmann, R. Luxenhofer, *Macromol. Rapid Comm.* **2012**, *19*, 1714.
[65] I. Shin, K. Park, *Org. Lett.* **2002**, *4*, 869.
[66] A. Cheguillaume, F. Lehardy, K. Bouget, M. Baudy-Floc'h, P. Le Grel, *J. Org. Chem.* **1999**, *64*, 2924.
[67] Y. Gao, T. Kodadek, *Chem. Biol.* **2013**, *20*, 360.
[68] B. K. Sarma, M. Yousufuddin, T. Kodadek, *Chem. Comm.* **2011**, *47*, 10590.
[69] B. K. Sarma, T. Kodadek, *ACS Comb. Sci.* **2012**, *14*, 558.
[70] F. Liu, A. G. Stephen, C. S. Adamson, K. Gousset, M. J. Aman, E. O. Freed, R. J. Fischer, T. R. Burke Jr., *Org. Lett.* **2006**, *8*, 5165.
[71] A. M. Rosales, H. K. Murnen, S. R. Kline, R. N. Zuckermann, R. A. Segalman, *Soft Matter* **2012**, *8*, 3673.
[72] Q. Sui, D. Borchardt, D. L. Rabenstein, *J. Am. Chem. Soc.* **2007**, *129*, 12042.
[73] A. Aditya, T. Kodadek, *ACS Comb. Sci.* **2012**, *14*, 164.
[74] S. Suwal, T. Kodadek, *Org. Biomol. Chem.* **2013**, *11*, 2088.
[75] D. G. Rivera, F. León, O. Concepción, F. E. Morales, L. A. Wessjohann, *Chemistry* **2013**, *19*, 6417.
[76] J. J. Diaz-Mochon, M. A. Fara, R. M. Sanchez-Martin, M. Bradley, *Tetrahedron Lett.* **2008**, *49*, 923.
[77] K. Peschko, A. Schade, S. B. Vollrath, U. Schwarz, B. Luy, C. Muhle-Goll, P. Weis, S. Bräse, *Chemistry* **2014**, *20*, 16273.
[78] K. Wüthrich, C. Grathwohl, *FEBS Lett.* **1974**, *43*, 337.
[79] J.-C. Horng, R. T. Raines, *Protein Sci.* **2006**, *15*, 74.
[80] J. A. Hodges, R. T. Raines, *Org. Lett.* **2006**, *8*, 4695.
[81] B. C. Gorske, B. L. Bastian, G. D. Geske, H. E. Blackwell, *J. Am. Chem. Soc.* **2007**, *129*, 8928.
[82] B. C. Gorske, J. R. Stringer, B. L. Bastian, S. A. Fowler, H. E. Blackwell, *J. Am. Chem. Soc.* **2009**, 16555.
[83] B. C. Gorske, R. C. Nelson, Z. S. Bowden, T. A. Kufe, A. M. Childs, *J. Org. Chem.* **2013**, *78*, 11172.
[84] B. Paul, G. L. Butterfoss, M. G. Boswell, M. L. Huang, R. Bonneau, C. Wolf, K. Kirshenbaum, *Org. Lett.* **2012**, *14*, 926.
[85] N. H. Shah, G. L. Butterfoss, K. Nguyen, B. Yoo, R. Bonneau, D. L. Rabenstein, K. Kirshenbaum, *J. Am. Chem. Soc.* **2008**, *130*, 166222.
[86] J. K. Pokorski, L. M. M. Jenkins, H. Feng, S. R. Durell, Y. Bai, D. H. Appella, *Org. Lett.* **2007**, *9*, 2381.
[87] O. Roy, C. Caumes, Y. Esvan, C. Didierjean, S. Faure, C. Taillefumier, *Org. Lett.* **2013**, *15*, 2246.
[88] C. Caumes, O. Roy, S. Faure, C. Taillefumier, *J. Am. Chem. Soc.* **2012**, *134*, 9553.
[89] P. Armand, K. Kirshenbaum, A. Falicov, R. L. Dunnbrack Jr., K. A. Dill, R. N. Zuckermann, F. E. Cohen, *Folding Des.* **1997**, *2*, 369.
[90] C. W. Wu, T. J. Sanborn, R. N. Zuckermann, A. E. Barron, *J. Am. Chem. Soc.* **2001**, *123*, 2958.
[91] C. W. Wu, K. Kirshenbaum, T. J. Sanborn, J. A. Patch, K. Huang, K. A. Dill, R. N. Zuckermann, A. E. Barron, *J. Am. Chem. Soc.* **2003**, *125*, 13525.
[92] H. M. Shin, C. M. Kang, M. H. Yoon, J. Seo, *Chem. Comm.* **2014**, *50*, 4465.
[93] J. Seo, A. E. Barron, R. N. Zuckermann, *Org. Lett.* **2010**, *12*, 492.
[94] B. C. Gorske, H. E. Blackwell, *J. Am. Chem. Soc.* **2006**, *128*, 14378.
[95] K. Huang, C. W. Wu, T. J. Sanborn, J. A. Patch, K. Kirshenbaum, R. N. Zuckermann, A. E. Barron, I. Radhakrishnan, *J. Am. Chem. Soc.* **2006**, *128*, 1733.
[96] S. A. Fowler, R. Luechapanichkul, H. E. Blackwell, *J. Org. Chem.* **2009**, *74*, 1440.
[97] J. A. Crapster, J. R. Stringer, I. A. Guzei, H. E. Blackwell, *Biopolymers* **2011**, *96*, 604.
[98] K. T. Nam, S. A. Shelby, P. H. Choi, A. B. Marciel, R. Chen, L. Tan, T. K. Chu, R. A. Mesch, B.-C. Lee, M. D. Connolly, C. Kisielowski, R. N. Zuckermann, *Nat. Mater.* **2010**, *9*, 454.
[99] M. T. Krejchi, E. D. Atkins, A. J. Waddon, M. J. Fournier, T. L. Mason, D. A. Tirrell, *Science* **1994**, *265*, 1427.
[100] J. A. Crapster, I. A. Guzei, H. E. Blackwell, *Angew. Chem. Int. Ed.* **2013**, *52*, 5079.
[101] C. Fetsch, R. Luxenhofer, *Polymers* **2013**, *5*, 112.
[102] C.-U. Lee, A. Li, K. Ghale, D. Zhang, *Macromolecules* **2013**, *46*, 8213.
[103] A. M. Rosales, H. K. Murnen, R. N. Zuckermann, R. A. Segalman, *Macromolecules* **2010**, *43*, 5627.
[104] S. H. Lahasky, X. Hu, D. Zhang, *ACS Macro Lett.* **2012**, *1*, 580.
[105] J. W. Robinson, C. Secker, S. Weidner, H. Schlaad, *Macromolecules* **2013**, *46*, 580.
[106] J. W. Robinson, H. Schlaad, *Chem. Comm.* **2012**, *48*, 7835.
[107] J. Sun, G. M. Stone, N. P. Balsara, R. N. Zuckermann, *Macromolecules* **2012**, *45*, 5151.
[108] J. Sun, A. A. Teran, X. Liao, N. P. Balsara, R. N. Zuckermann, *J. Am. Chem. Soc.* **2013**, *135*, 14119.
[109] J. Sun, A. A. Teran, X. Liao, N. P. Balsara, R. N. Zuckermann, *J. Am. Chem. Soc.* **2014**, *136*, 2070.
[110] J. Sun, X. Liao, A. M. Minor, N. P. Balsara, R. N. Zuckermann, *J. Am. Chem. Soc.* **2014**, *136*, 14990.
[111] L. Guo, D. Zhang, *J. Am. Chem. Soc.* **2009**, *131*, 18072.
[112] A. M. Rosales, B. L. McCulloch, R. N. Zuckermann, R. A. Segalman, *Macromolecules* **2012**, *45*, 6027.
[113] W. van Zoelen, R. N. Zuckermann, R. A. Segalman, *Macromolecules* **2012**, *45*, 7072.
[114] I. Banerjee, R. C. Pangule, R. S. Kane, *Adv. Mater.* **2011**, *23*, 690.
[115] K. H. A. Lau, C. Ren, S. H. Park, I. Szleifer, P. B. Messersmith, *Langmuir* **2012**, *28*, 2288.
[116] K. H. A. Lau, C. Ren, T. S. Sileika, S. H. Park, I. Szleifer, P. B. Messersmith, *Langmuir* **2012**, *28*, 16099.
[117] A. R. Statz, A. E. Barron, P. B. Messersmith, *Soft Matter* **2008**, *4*, 131.
[118] K. H. A. Lau, T. S. Sileika, S. H. Park, A. M. L. Sousa, P. Burch, I. Szleifer, P. B. Messersmith, *Adv. Mater. Interfaces* **2015**, *2*.
[119] H. O. Ham, S. H. Park, J. W. Kurutz, I. G. Szleifer, P. B. Messersmith, *J. Am. Chem. Soc.* **2013**, *135*, 13015.
[120] J. Y. Ryu, I. T. Song, K. H. A. Lau, P. B. Messersmith, T.-Y. Yoon, H. Lee, *ACS Appl. Mater. Interfaces* **2014**, *6*, 3553.
[121] F. Costa, I. F. Carvalho, R. C. Montelaro, P. Gomes, M. C. L. Martins, *Acta Biomater.* **2011**, *7*, 1431.
[122] N. P. Chongsiriwatana, J. A. Patch, A. M. Czyzewski, M. T. Dohm, A. Ivankin, D. Gidalevitz, R. N. Zuckermann, A. E. Barron, *Proc. Natl. Acad. Sci. U. S. A.* **2008**, *105*, 2794.
[123] T. Godballe, L. L. Nilsson, P. D. Petersen, H. Jenssen, *Chem. Biol. Drug Des.* **2011**, *77*, 107.

[124] A. R. Statz, J. P. Park, N. P. Chongsiriwatana, A. E. Barron, P. B. Messersmith, *Biofouling* **2008**, *24*, 439.
[125] T. J. Ward, K. D. Ward, *Anal. Chem.* **2010**, *82*, 4712.
[126] H. Wu, T. Liang, C. Yin, Y. Jin, Y. Ke, X. Liang, *Analyst* **2011**, *136*, 4409.
[127] H. Wu, K. Li, H. Yu, Y. Ke, X. Liang, *J. Chromatogr. A* **2013**, *1281*, 155.
[128] H. Wu, G. Song, D. Wang, H. Yu, Y. Ke, X. Liang, *J. Chromatogr. A* **2013**, *1298*, 152.
[129] H. Wu, D. Wang, G. Song, Y. Ke, X. Liang, *J. Sep. Sci.* **2014**, *37*, 934.
[130] R. Frank, *Tetrahedron* **1992**, *48*, 9217.
[131] H. E. Blackwell, *Curr. Opin. Chem. Biol.* **2006**, *10*, 203.
[132] J. A. Hong, D. V Neel, D. Wassaf, F. Caballero, A. N. Koehler, *Curr. Opin. Chem. Biol.* **2014**, *18*, 21.
[133] J. Voskuhl, J. Brinkmann, P. Jonkheijm, *Curr. Opin. Chem. Biol.* **2014**, *18*, 1.
[134] M. M. Reddy, T. Kodadek, *Proc. Natl. Acad. Sci. U. S. A.* **2005**, *102*, 12672.
[135] Y.-U. Kwon, T. Kodadek, *Chem. Comm.* **2008**, 5704.
[136] H.-S. Lim, M. M. Reddy, X. Xiao, J. Wilson, R. Wilson, S. Connell, T. Kodadek, *Bioorg. Med. Chem. Lett.* **2009**, *19*, 3866.
[137] L. P. Labuda, A. Pushechnikov, M. D. Disney, *ACS Chem. Biol.* **2009**, *4*, 299.
[138] G. Maayan, M. D. Ward, K. Kirshenbaum, *Chem. Comm.* **2009**, *1*, 56.
[139] I. Izzo, G. Ianniello, C. De Cola, B. Nardone, L. Erra, G. Vaughan, C. Tedesco, F. De Riccardis, *Org. Lett.* **2013**, *15*, 598.
[140] C. De Cola, G. Fiorillo, A. Meli, S. Aime, E. Gianolio, I. Izzo, F. De Riccardis, *Org. Biomol. Chem.* **2014**, *12*, 424.
[141] D. M. Nalband, B. P. Warner, N. H. Zahler, K. Kirshenbaum, *Pept. Sci.* **2014**, *102*, 407.
[142] M. B. Francis, T. F. Jamison, E. N. Jacobsen, *Curr. Opin. Chem. Biol.* **1998**, *2*, 422.
[143] M. B. Francis, N. S. Finney, E. N. Jacobsen, *J. Am. Chem. Soc.* **1996**, *118*, 8983.
[144] R. D. Hancock, A. E. Martell, *Chem. Rev.* **1989**, *89*, 1875.
[145] F. C. Meldrum, H. Cölfen, *Chem. Rev.* **2008**, *108*, 4332.
[146] C.-L. Chen, J. Qi, R. N. Zuckermann, J. J. DeYoreo, *J. Am. Chem. Soc.* **2011**, *133*, 5214.
[147] M. L. Huang, D. Ehre, Q. Jiang, C. Hu, K. Kirshenbaum, M. D. Ward, *Proc. Natl. Acad. Sci. U. S. A.* **2012**, *109*, 19922.
[148] M. Cusack, A. Freer, *Chem. Rev.* **2008**, *108*, 4433.
[149] N. A. J. M. Sommerdijk, G. de With, *Chem. Rev.* **2008**, *108*, 4499.
[150] C.-L. Chen, J. Qi, J. Tao, R. N. Zuckermann, J. J. DeYoreo, *Sci. Rep.* **2014**, *4*, 6266.
[151] V. Haridas, S. Naik, *RSC Adv.* **2013**, *3*, 14199.
[152] C. A. Koh, E. D. Sloan, A. K. Sum, D. T. Wu, *Annu. Rev. Chem. Biomol. Eng.* **2011**, *2*, 237.
[153] F. T. Reyes, M. A. Kelland, N. Kumar, L. Jia, *Energy Fuels.* **2015**, *29*, 695 .
[154] W. Lu, Z. Wei, Z.-Y. Gu, T.-F. Liu, J. Park, J. Park, J. Tian, M. Zhang, Q. Zhang, T. Gentle III, M. Bosch, H.-C. Zhou, *Chem. Soc. Rev.* **2014**, *43*, 5561.
[155] P. Falcaro, R. Ricco, C. M. Doherty, K. Liang, A. J. Hill, M. J. Styles, *Chem. Soc. Rev.* **2014**, *43*, 5513.
[156] S. B. L. Vollrath, C. Hu, S. Bräse, K. Kirshenbaum, *Chem. Comm.* **2013**, *49*, 2317.
[157] X. Gao, H. Matsui, *Adv. Mater.* **2005**, *17*, 2037.
[158] M. R. Ghadiri, J. R. Granja, R. A. Milligan, D. E. McRee, N. Khazanovich, *Nature* **1993**, *366*, 324.
[159] G. L. Butterfoss, B. Yoo, J. N. Jaworski, I. Chorny, K. A. Dill, R. N. Zuckermann, R. Bonneau, K. Kirshenbaum, V. A. Voelz, *Proc. Natl. Acad. Sci. U. S. A.* **2012**, *109*, 14320.
[160] T. Aida, E. W. Meijer, S. I. Stupp, *Science* **2012**, *335*, 813.
[161] E. Busseron, Y. Ruff, E. Moulin, N. Giuseppone, *Nanoscale* **2013**, *5*, 7098.
[162] H.-A. Klok, S. Lecommandoux, *Adv. Mater.* **2001**, *13*, 1217.
[163] R. C. Elgersma, G. E. Mulder, J. A. W. Kruijtzer, G. Posthuma, D. T. S. Rijkers, R. M. J. Liskamp, *Bioorg. Med. Chem. Lett.* **2007**, *17*, 1837.
[164] H. K. Murnen, A. M. Rosales, J. N. Jaworski, R. A. Segalman, R. N. Zuckermann, *J. Am. Chem. Soc.* **2010**, *132*, 16112.
[165] J. J. L. M. Cornelissen, M. Fischer, N. A. J. M. Sommerdijk, R. J. M. Nolte, *Science* **1998**, *280*, 1427.
[166] N. A. Peppas, J. Z. Hilt, A. Khademhosseini, R. Langer, *Adv. Mater.* **2006**, *18*, 1345.
[167] Z. Wu, M. Tan, X. Chen, Z. Yang, L. Wang, *Nanoscale* **2012**, *4*, 3644.
[168] H. P. R. Mangunuru, H. Yang, G. Wang, *Chem. Comm.* **2013**, *49*, 4489.
[169] M. L. Hebert, D. S. Shah, P. Blake, J. P. Turner, S. L. Servoss, *Org. Biomol. Chem.* **2013**, *11*, 4459.
[170] M. L. Hebert, D. S. Shah, P. Blake, S. L. Servoss, *Coatings* **2013**, *3*, 98.
[171] B. Sanii, R. Kudirka, A. Cho, N. Venkateswaran, G. K. Olivier, A. M. Olson, H. Tran, R. M. Harada, L. Tan, R. N. Zuckermann, *J. Am. Chem. Soc.* **2011**, *133*, 20808.
[172] R. Kudirka, H. Tran, B. Sanii, K. T. Nam, P. H. Choi, N. Venkateswaran, R. Chen, S. Whitelam, R. N. Zuckermann, *Pept. Sci.* **2011**, *96*, 586.
[173] E. J. Robertson, G. K. Olivier, M. Qian, C. Proulx, R. N. Zuckermann, G. L. Richmond, *Proc. Natl. Acad. Sci. U. S. A.* **2014**, *111*, 13284.
[174] B. Sanii, T. K. Haxton, G. K. Olivier, A. Cho, B. Barton, C. Proulx, S. Whitelam, R. N. Zuckermann, *ACS Nano* **2014**, *8*, 11674.
[175] T. K. Haxton, R. V. Mannige, R. N. Zuckermann, S. Whitelam, *J. Chem. Theory Comput.* **2015**, *11*, 303.
[176] G. K. Olivier, A. Cho, B. Sanii, M. D. Connolly, H. Tran, R. N. Zuckermann, *ACS Nano* **2013**, *7*, 9276.
[177] M. E. Davis, *Curr. Opin. Biotechnol.* **2002**, *13*, 128.
[178] J. A. Doudna, E. Charpentier, *Science* **2014**, *346*, 1258096.
[179] D. W. Pack, A. S. Hoffman, S. Pun, P. S. Stayton, *Nat. Rev. Drug Discov.* **2005**, *4*, 581.
[180] T. R. Pearce, K. Shroff, E. Kokkoli, *Adv. Mater.* **2012**, *24*, 3803.
[181] C.-Y. Huang, T. Uno, J. E. Murphy, S. Lee, J. D. Hamer, J. A. Escobedo, F. E. Cohen, R. Radhakrishnan, V. Dwarki, R. N. Zuckermann, *Chem. Biol.* **1998**, *5*, 345.
[182] B. A. Lobo, J. A. Vetro, D. M. Suich, R. N. Zuckermann, C. R. Middaugh, *J. Pharm. Sci.* **2003**, *92*, 1905.
[183] Y. Utku, E. Dehan, O. Ouerfelli, F. Piano, R. N. Zuckermann, M. Pagano, K. Kirshenbaum, *Mol. BioSyst.* **2006**, *2*, 312.
[184] Y. U. Konca, K. Kirshenbaum, R. N. Zuckermann, *Int. J. Nanomedicine* **2014**, *9*, 2271.
[185] C. W. Wu, S. L. Seurynck, K. Y. C. Lee, A. E. Barron, *Chem. Biol.* **2003**, *10*, 1057.
[186] J. A. Patch, A. E. Barron, *J. Am. Chem. Soc.* **2003**, *125*, 12092.
[187] N. J. Brown, M. T. Dohm, J. Bernardino de la Serna, A. E. Barron, *Biophys. J.* **2011**, *101*, 1076.
[188] S. L. Seurynck, J. A. Patch, A. E. Barron, *Chem. Biol.* **2005**, *12*, 77.
[189] S. L. Seurynck-Servoss, M. T. Dohm, A. E. Barron, *Biochemistry* **2006**, *45*, 11809.
[190] M. T. Dohm, N. J. Brown, S. L. Seurynck-Servoss, J. Bernardino de la Serna, A. E. Barron, *Biochim. Biophys. Acta* **2010**, *1798*, 1663.
[191] M. T. Dohm, S. L. Seurynck-Servoss, J. Seo, R. N. Zuckermann, A. E. Barron, *Pept. Sci.* **2009**, *92*, 538.
[192] T. S. Burkoth, E. Beausoleil, S. Kaur, D. Tang, F. E. Cohen, R. N. Zuckermann, *Chem. Biol.* **2002**, *9*, 647.
[193] B.-C. Lee, R. N. Zuckermann, K. A. Dill, *J. Am. Chem. Soc.* **2005**, *127*, 10999.

Adv. Mater. **2015**,
DOI: 10.1002/adma.201500275

[194] H. K. Murnen, A. R. Khokhlov, P. G. Khalatur, R. A. Segalman, R. N. Zuckermann, *Macromolecules* **2012**, *45*, 5229.
[195] A. R. Khoklov, P. G. Khalatur, *Phys. Rev. Lett.* **1999**, *82*, 3456.
[196] B. C. Lee, T. K. Chu, K. A. Dill, R. N. Zuckermann, *J. Am. Chem. Soc.* **2008**, *130*, 8847.
[197] M. Klemba, L. Regan, *Biochemistry* **1995**, *34*, 10094.
[198] P. M. Levine, T. W. Craven, R. Bonneau, K. Kirshenbaum, *Org. Lett.* **2014**, *16*, 512.
[199] X. Chen, K. Ding, N. Ayres, *Polym. Chem.* **2011**, *2*, 2635.
[200] Y. Zhang, C. Xu, H. Y. Lam, C. L. Lee, X. Li, *Proc. Natl. Acad. Sci. U. S. A.* **2013**, *110*, 6657.
[201] B.-C. Lee, R. N. Zuckermann, *ACS Chem Biol.* **2011**, *6*, 1367.
[202] J. E. Hudak, C. R. Bertozzi, *Chem. Biol. (Oxford, U. K.)* **2014**, *21*, 16.
[203] L. L. Kiessling, J. C. Grim, *Chem. Soc. Rev.* **2013**, *42*, 4476.
[204] N. C. Reichardt, M. Martín-Lomas, S. Penadés, *Chem. Soc. Rev.* **2013**, *42*, 4358.
[205] X. Chen, O. Ramström, M. Yan, *Nano Res.* **2014**, *7*, 1381.
[206] U. K. Saha, R. Roy, *Tetrahedron Lett.* **1995**, *36*, 3635.
[207] T. Szekely, O. Roy, S. Faure, C. Taillefumier, *Eur. J. Org. Chem.* **2014**, *2014*, 5641.
[208] D. Comegna, F. De Riccardis, *Org. Lett.* **2009**, *11*, 3898.
[209] S. N. Khan, A. Kim, R. H. Grubbs, Y.-U. Kwon, *Org. Lett.* **2012**, *14*, 2952.
[210] J. Seo, N. Michaelian, S. C. Owens, S. T. Dashner, A. J. Wong, A. E. Barron, M. R. Carrasco, *Org. Lett.* **2009**, *11*, 5210.
[211] A. S. Norgren, C. Budke, Z. Majer, C. Heggemann, T. Koop, N. Sewald, *Synthesis* **2009**, 488.
[212] A. Singhamahapatra, L. Sahoo, D. Loganathan, *J. Org. Chem.* **2013**, *78*, 10329.
[213] A. Singhamahapatra, L. Sahoo, B. Varghese, D. Loganathan, *RSC Adv.* **2014**, *4*, 18038.
[214] Y. Huang, L. Taylor, X. Chen, N. Ayres, *J. Polym. Sci., Part A: Polym. Chem.* **2013**, *51*, 5230.
[215] Y. Li, J. Rodrigues, H. Tomás, *Chem. Soc. Rev.* **2012**, *41*, 2193.
[216] A. Stein, R. Mosca, P. Aloy, *Curr. Opin. Struct. Biol.* **2011**, *21*, 200.
[217] B. R. Brooks, R. E. Bruccoleri, B. D. Olafson, D. J. States, S. Swaminathan, M. Karplus, *J. Comput. Chem.* **1983**, *4*, 187.
[218] B. R. Brooks, C. L. Brooks III, A. D. Mackerell Jr., L. Nilsson, R. J. Petrella, B. Roux, Y. Won, G. Archontis, C. Bartels, S. Boresch, A. Caflisch, L. Caves, Q. Cui, A. R. Dinner, M. Feig, S. Fischer, J. Gao, M. Hodoscek, W. Im, K. Kuczera, T. Lazaridis, J. Ma, V. Ovchinnikov, E. Paci, R. W. Pastor, C. B. Post, J. Z. Pu, M. Schaefer, B. Tidor, R. M. Venable, H. L. Woodcock, X. Wu, W. Yang, D. M. York, M. Karplus, *J. Comput. Chem.* **2009**, *30*, 1545.
[219] K. W. Kaufmann, G. H. Lemmon, S. L. Deluca, J. H. Sheehan, J. Meiler, *Biochemistry* **2010**, *49*, 2987.
[220] G. L. Butterfoss, P. D. Renfrew, B. Kuhlman, K. Kirshenbaum, R. Bonneau, *J. Am. Chem. Soc.* **2009**, *131*, 16798.
[221] D. T. Mirijanian, R. V Mannige, R. N. Zuckermann, S. Whitelam, *J. Comput. Chem.* **2014**, *35*, 360.
[222] U. Sternberg, E. Birtalan, I. Jakovkin, B. Luy, U. Schepers, S. Bräse, C. Muhle-Goll, *Org. Biomol. Chem.* **2013**, *11*, 640.
[223] K. Drew, P. D. Renfrew, T. W. Craven, G. L. Butterfoss, F.-C. Chou, S. Lyskov, B. N. Bullock, A. Watkins, J. W. Labonte, M. Pacella, K. P. Kilambi, A. Leaver-Fay, B. Kuhlman, J. J. Gray, P. Bradley, K. Kirshenbaum, P. S. Arora, R. Das, R. Bonneau, *PLoS One* **2013**, *8*, e67051.
[224] P. D. Renfrew, T. W. Craven, G. L. Butterfoss, K. Kirshenbaum, R. Bonneau, *J. Am. Chem. Soc.* **2014**, *136*, 8772.